doi:10.1093/brain/awl170 Brain (2006), 129, 1984–1992

Selective COX-2 inhibitor celecoxib prevents experimental autoimmune encephalomyelitis through COX-2-independent pathway

Katsuichi Miyamoto,[1,2] Sachiko Miyake,[1] Miho Mizuno,[1] Nobuyuki Oka,[3] Susumu Kusunoki[2] and Takashi Yamamura[1]

[1]Department of Immunology, National Institute of Neuroscience, NCNP, Tokyo, [2]Department of Neurology, Kinki University School of Medicine, Osaka and [3]Department of Rehabilitation Medicine, Minami-kyoto National Hospital, Kyoto, Japan

Correspondence to: Sachiko Miyake, Department of Immunology, National Institute of Neuroscience, NCNP, Kodaira, Tokyo 187-8502, Japan
E-mail: miyake@ncnp.go.jp

Cyclooxygenase (COX) is a key enzyme of arachidonic acid metabolism and exists as two distinct isoforms. COX-1 is constitutively expressed in most tissues, whereas COX-2 is inducibly expressed at the site of inflammation. Selective inhibitors of COX-2 have been developed and have been used as anti-inflammatory agents. Here, we show that a new-generation COX-2 inhibitor, celecoxib, inhibited experimental autoimmune encephalomyelitis (EAE). Celecoxib, but not other COX-2 inhibitors such as nimesulid, prevented myelin oligodendrocyte glycoprotein (MOG) induced EAE when administrated orally on the day of disease induction. Moreover, celecoxib inhibited EAE in COX-2-deficient mice, indicating that celecoxib inhibited EAE in a COX-2-independent manner. In celecoxib-treated mice, interferon-γ (IFN-γ) production from MOG-specific T cells was reduced and MOG-specific IgG1 was elevated compared with vehicle-treated mice. Infiltration of inflammatory cells into the central nervous system and the expression of adhesion molecules, P-selectin and intercellular adhesion molecule-1 (ICAM-1), and a chemokine, monocyte chemoattractant peptide-1 (MCP-1), were inhibited when mice were treated with celecoxib. These results suggest that celecoxib may be useful as a new additional therapeutic agent for multiple sclerosis.

Keywords: COX-2 inhibitor; celecoxib; experimental autoimmune encephalomyelitis; multiple sclerosis

Abbreviations: CMC = carboxymethylcellulose; COX = cyclooxygenase; EAN = experimental autoimmune neuritis; EAE = experimental autoimmune encephalomyelitis; ELISA = enzyme-linked immunosorbent assay; ICAM-1 = intercellular adhesion molecule-1; IFN = interferon; IL = interleukin; LN = lymph node; MCP-1 = monocyte chemoattractant peptide-1; MOG = myelin oligodendrocyte glycoprotein; PBS = phosphate-buffered saline

Received February 6, 2006. Revised April 11, 2006. Accepted May 31, 2006. Advance Access publication July 10, 2006

Introduction

Cyclooxygenase (COX) catalyses the conversion of arachidonic acid to prostaglandins and has two isoforms, COX-1 and COX-2 (Vane *et al.*, 1994; Warner and Mitchell, 2004). COX-1 is constitutively expressed in most tissues and produces prostaglandins involved in maintenance of the gastric mucosa, regulation of renal blood flow and platelet aggregation. On the other hand, COX-2 is inducibly expressed in cells involved in inflammation and in neoplastic tissues by proinflammatory and mitogenic stimuli, and is primarily responsible for the synthesis of prostanoids involved in acute and chronic inflammation (Xie *et al.*, 1997). COX-2 therefore appears to be a suitable target for the anti-inflammatory effects of non-steroidal anti inflammatory drugs. These findings have provided the rationale for the development of selective inhibitors of COX-2.

Celecoxib is a new generation of highly specific COX-2 inhibitors that have been approved for the treatment of rheumatoid arthritis and other inflammatory diseases. The selectivity of COX-2 inhibition is much higher than traditional COX-2 inhibitors (Penning *et al.*, 1997). Furthermore, celecoxib has been shown to exert a potent anti-tumour effect. Interestingly, the anti-tumour effect by celecoxib

has been reported via both COX-2-dependent and COX-2-independent mechanisms (Grosch *et al.*, 2001). For example, cell cycle arrest and apoptosis of various kinds of cells induced by celecoxib appeared to be COX-2-independent effects (Hsu *et al.*, 2000; Arico *et al.*, 2002; Liu *et al.*, 2004).

Experimental autoimmune encephalomyelitis (EAE) is a widely used animal model for multiple sclerosis that can be induced by immunization with myelin antigens such as myelin oligodendrocyte glycoprotein (MOG). EAE is mediated primarily by $CD4^+$ Th1 T cells producing interferon-γ (IFN-γ) and tumour necrosis factor-α (TNF-α) (Nicholson and Kuchroo, 1996; Kumar *et al.*, 1997; Zhang *et al.*, 1997). COX-2 is expressed in neurons and endothelial cells in healthy brain. In rats with EAE, the expression of COX-2 was reported to be upregulated in endothelial cells in inflammatory lesions. In addition, non-selective COX-2 inhibitors have been reported to moderately ameliorate EAE (Prosiegel *et al.*, 1989; Weber *et al.*, 1991; Simmons *et al.*, 1992), suggesting that COX-2 may have an important role in the pathogenesis of EAE (Deininger and Schluesener, 1999). Furthermore, we recently demonstrated that COX-2 inhibitors suppress experimental autoimmune neuritis (EAN), a model of Guillain–Barré syndrome, which is also characterized as a $CD4^+$-Th1 T-cell-mediated autoimmune neurological disease model similar to EAE (Miyamoto *et al.*, 1998, 1999, 2002). These findings led us to investigate the effect of COX-2 inhibitors on EAE.

In the present study, we found that celecoxib greatly suppressed EAE in comparison with traditional COX-2 inhibitors. Furthermore, we have demonstrated that celecoxib inhibited EAE by inhibiting Th1 response of autoreactive T cells and that this inhibition was COX-2-independent. Finally, we demonstrated that celecoxib prevented cell entry into the CNS in association with the inhibition of the expression of P-selectin, intercellular adhesion molecule-1 (ICAM-1) and monocyte chemoattractant peptide-1 (MCP-1). These results highlighted the COX-2-independent therapeutic potential of celecoxib for multiple sclerosis.

Material and methods

Mouse

Wild-type C57BL/6 (B6) mice were purchased from Clea Japan (Tokyo, Japan). COX-2-deficient mice ($COX\text{-}2^{-/-}$) have been backcrossed to B6 background for more than five generations and were purchased from Taconic (Germantown, NY, USA). These mice were maintained under specific pathogen-free conditions.

Induction of EAE

For induction of EAE, mice were immunized (5–10 mice per group) subcutaneously in flanks with 100 μg of MOG_{35-55} peptide (MEVGWYRSPFSRVVHLYRNGK) in 0.1 ml phosphate-buffered saline (PBS) and 0.1 ml complete Freund's adjuvant (CFA) containing 1 mg *Mycobacterium tuberculosis* H37Ra (Difco Laboratories, Detroit, MI, USA) and were injected intravenously with 200 ng of pertussis toxin (List Biological Laboratories, Campbell, CA, USA) on the day of immunization and 2 days later.

Clinical assessment of EAE

EAE was scored on the following scale: 0 = no clinical signs; 1 = partial loss of tail tonicity; 2 = completely limp tail and abnormal gait; 3 = partial hindlimb paralysis; 4 = complete hindlimb paralysis; and 5 = fore- and hindlimb paralysis or moribund state.

Treatment with COX-2 inhibitors

Mice were orally administered 5 μg/g of COX-2 inhibitor, celecoxib (Searle, St Louis, MO, USA) (Penning *et al.*, 1997), nimesulid (Nakarai Tesque, Kyoto, Japan) (Nakatsuji *et al.*, 1996), or indomethacin (Nakarai Tesque) in 0.5% carboxymethylcellulose (CMC) via a feeding cannula every 2 days. Control mice were orally administered vehicle (0.5% CMC) alone.

Measurement of MOG_{35-55}-specific IgG1 and IgG2a titres

Enzyme-linked immunosorbent assay (ELISA) plates (Sumitomo, Tokyo, Japan) were coated with 10 μg/ml MOG_{35-55} in PBS overnight at 4°C. After blocking with 2% bovine serum albumin (BSA) in PBS, different dilutions of the serum from animals at Day 30 after immunization, or normal mice or PBS were added to the plate. MOG_{35-55}-specific antibodies were detected using biotin-labelled anti-IgG1 and anti-IgG2a antibodies (Vector Laboratories, Burlingame, CA, USA). After adding streptavidin-peroxidase (BD Biosciences, San Jose, CA, USA) and a substrate, plates were read at OD_{450} values.

MOG_{35-55}-specific T-cell proliferation assay

On Day 11 after immunization with MOG_{35-55}, draining lymph nodes (LN) were harvested and single cell suspensions were prepared. Cells were cultured in RPMI1640 medium (Gibco, Grand Island, NY, USA) supplemented with 5×10^{-5} M 2-mercaptoethanol, 2 mM L-glutamine, 100 U/ml penicillin and streptomycin and 1% autologous mouse serum, and seeded onto 96-well flat-bottom plates (1×10^6 cells/well). The cells were stimulated with peptide for 72 h at 37°C in a humidified air condition with 5% CO_2. To measure cellular proliferation, [^{3}H]-thymidine was added (1 μCi/well) and uptake of the radioisotope during the final 18 h of culture was counted with a beta-1205 counter (Pharmacia, Uppsala, Sweden). To evaluate proliferative responses of LN cells to peptide, we determined the Δc.p.m. value for cells in each well by subtracting the background c.p.m.

Detection of cytokines and chemokine

LN cells from the MOG_{35-55}-immunized mice were cultured in the standard medium in 96-well flat-bottom plates at 1×10^6/well for 48 h in the presence of the different concentrations of MOG_{35-55}. The concentrations of IFN-γ, interleukin-4 (IL-4) and IL-10 in the supernatants were measured by using a sandwich ELISA following the protocol provided by BD Biosciences. A chemokine, MCP-1, in the serum from mice on Day 7, 10 and 14 after induction of EAE was also measured by using a sandwich ELISA following the protocol provided by BD Biosciences. All reagents, including recombinant mouse cytokines, chemokine and antibodies were purchased from BD Biosciences.

Analysis of infiltrating cells isolated from CNS

Mice were anaesthetized with diethyl ether on Day 14 after induction of EAE. After perfusion with PBS, brain and spinal cord were removed and homogenized. After washing with PBS, mononuclear cells were isolated using Ficoll gradient (Amersham Biosciences, Piscataway, NJ, USA) (Krakowski *et al.*, 1997). The cells were stained with APC-labelled anti-CD3 antibody, fluoroisothiocyanate (FITC) labelled anti-CD4 or CD8 or CD19 antibody (BD Biosciences) and were analysed by flow cytometer (BD FACS Calibur). Apoptosis of lymphocytes was analysed by using Annexin-5 apoptosis kit (BD Biosciences).

Pathological analysis

The brain and spinal cord were removed on Day 7, 10 and 14 after induction of EAE. Ten-micrometre frozen sections were fixed with acetone and stained with haematoxylin and eosin (HE), Luxol fast blue or antibodies of adhesion molecule ICAM-1 (CD54), vascular cell adhesion molecule-1 (VCAM-1: CD106), E-selectin (CD62E) and P-selectin (CD62P) (BD Biosciences), following the protocol provided by BD Biosciences.

Statistics

For statistic analysis, non-parametric Mann–Whitney *U*-test was used to calculate significant levels for all measurements. Values of $P < 0.05$ were considered statistically significant.

Results

Celecoxib inhibits EAE

To examine the effect of celecoxib on the development of EAE, we first administered celecoxib at the time of immunization with MOG_{35-55}. Oral administration of celecoxib reduced the incidence of disease and suppressed maximum EAE score and cumulative score compared with the control group (Fig. 1A, Table 1). Histological comparison between the thoracic region of the spinal cord demonstrated reduced monocyte infiltration and demyelination in cerecoxib-treated mice compared with vehicle-treated mice (Fig. 2A–D). Celecoxib was also effective in reducing the severity of disease when administered at Day 8

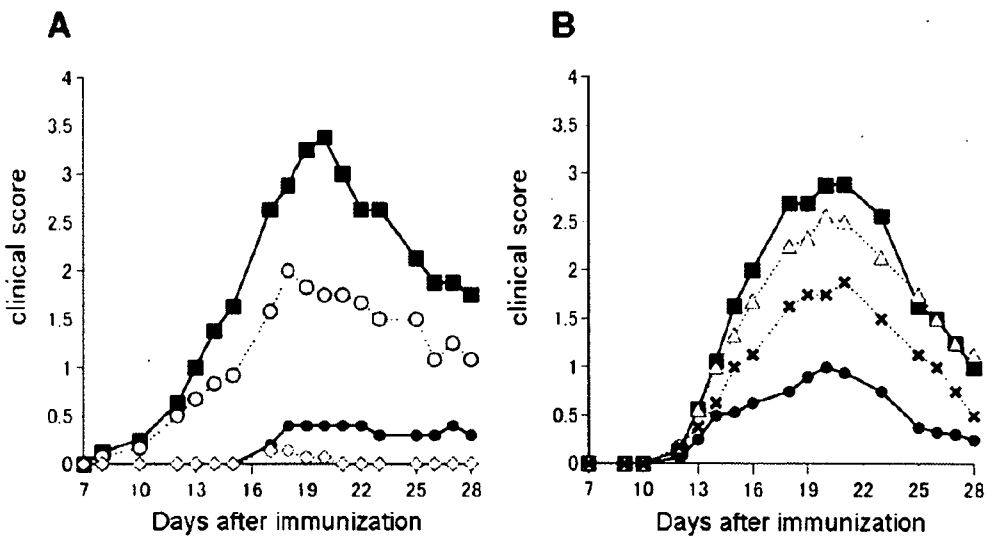

Fig. 1 Effect of celecoxib on actively induced EAE. EAE was induced in female B6 mice by immunization with MOG_{35-55} in CFA as described in Material and methods. (**A**) Mice were orally administered 5 μg/g (closed circles) or 10 μg/g (open diamond) of celecoxib starting from the day of the immunization, or with 5 μg/g of celecoxib starting from 8 days after the immunization (open circles). Control mice were administered vehicle alone (closed squares). Statistical analysis is shown in Table 1. (**B**) Mice were orally administered 5 μg/g of celecoxib (closed circles) or nimesulid (open triangle) or indomethacin (crosses) every 2 days from the day of EAE induction. Control mice were administered vehicle alone (closed squares). Statistical analysis is shown in Table 2. One representative experiment of two independent experiments is expressed as mean ± SEM.

Table 1 Clinical scores of EAE treated with celecoxib

	Max. score	Day of onset	Incidence (%)	Cumulative score
Control (CMC)	3.50 ± 0.20	12.50 ± 1.56	100 (10/10)	33.00 ± 5.05
Celecoxib 10 μg/g	0.14 ± 0.05*	17.50 ± 0.50	20.0 (2/10)	0.42 ± 0.04*
Celecoxib 5 μg/g	0.40 ± 0.40*	17.00 ± 0.00	20.0 (2/10)	3.80 ± 3.80*
Celecoxib 5 μg/g (from Day 8)	2.42 ± 0.57	14.20 ± 1.83	83.3 (10/12)	20.17 ± 5.22

Four groups of mice were immunized with MOG_{35-55} peptide for induction of EAE. The control CMC solution, 5 or 10 μg/g of celecoxib diluted in CMC, was orally injected via a cannula every 2 days starting from Day 0 or 8 after induction of EAE. Mean ± SEM of the following parameters are shown: maximum score of EAE (Max. score), the days of EAE onset, incidence of paralysed mice among sensitized mice (Incidence) and summation of the clinical scores from Day 0 to 30 (Cumulative score). *$P < 0.05$ versus control.

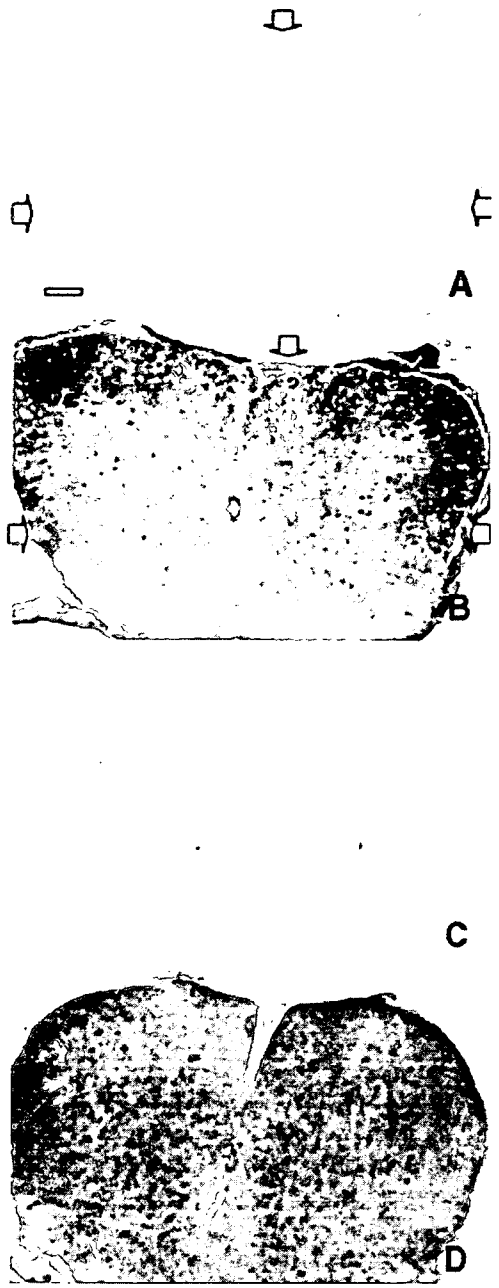

Fig. 2 Histopathological assessment of the CNS region in EAE-induced mice. Brains and spinal cords from EAE mice were removed on Day 14 after immunization as described in Material and methods. Thinly sliced (10 μm) frozen sections of the brains obtained from vehicle-treated mice (**A** and **B**) or celecoxib-treated mice (**C** and **D**) were stained with haematoxylin and eosin (**B** and **D**), or Luxol fast blue (**A** and **C**).

post-EAE-induction. Although indomethacin suppressed EAE to some extent, all mice died around Day 30 after immunization owing to intestinal ulcer. In contrast, oral administration of nimesulid, another COX-2 inhibitor, did not suppress either the incidence or the severity of EAE (Fig. 1B). Composite data from experiments is shown in Tables 1 and 2.

Celecoxib inhibits MOG-specific Th1 response

To determine the mechanisms by which celecoxib inhibits EAE, we examined the level of MOG-specific IgG1 and IgG2a in the serum samples collected from individual EAE-induced mice on Day 30. It is generally accepted that elevation of antigen-specific IgG2a antibody results from augmentation of a Th1 immune response to the antigen, whereas a higher level of IgG1 antibody would reflect a stronger Th2 response to the antigen. There was a significant elevation of the level of MOG_{35-55}-specific IgG1 and a slight reduction in the level of MOG-specific IgG2a in celecoxib-treated group compared with vehicle-treated group (Fig. 3A). In contrast, there was no significant difference in the level of either IgG1 or IgG2a in nimesulid-treated mice compared with vehicle-treated group (Fig. 3B).

To further investigate the response of T cells to MOG_{35-55} in celecoxib-treated mice, we examined the proliferative response and cytokine production of draining LN cells *in vitro*. Mice were immunized with MOG_{35-55} and were administered celecoxib or vehicle on the day of immunization. Ten days after immunization, draining LN cells were collected and cultured with MOG_{35-55} peptide. As shown in Fig. 4A, there was no significant difference in a proliferative response of MOG-reactive T cells between celecoxib-treated and vehicle-treated groups. We next examined the levels of cytokines in the culture supernatant by ELISA. The level of IFN-γ was reduced in the culture supernatants of LN cells obtained from mice treated with celecoxib compared with that from control mice (Fig. 4B). IL-4 and IL-10 were not detected in either culture supernatant. These results indicate that celecoxib reduces Th1 cytokine production from MOG-reactive T cells.

Celecoxib prevents EAE even in COX-2-deficient mice

Since another COX-2 inhibitor, nimesulid, did not have the inhibitory effect on EAE, we examined whether celecoxib could inhibit EAE in COX-2-deficient mice. As shown in Fig. 5A, the maximum EAE score, the day of onset and the severity of EAE were not significantly different between COX-$2^{-/-}$ and wild-type mice. Administration of celecoxib prevented the development of EAE in COX-$2^{-/-}$ mice as well as in wild-type mice. Consistent with the severity of EAE, the levels of MOG-specific IgG1 and IgG2a in COX-$2^{-/-}$ mice were not different compared with wild-type B6 mice (Fig. 5B). Moreover, celecoxib treatment increased the level of MOG-specific IgG1 even in COX-$2^{-/-}$ mice, resulting in the elevation of IgG1 : IgG2a ratio similar to that in wild-type mice (CMC = 0.29, celecoxib = 3.00) and COX-$2^{-/-}$ mice (CMC = 0.42, celecoxib = 2.52). These results indicate that the effect on the inhibition of EAE

Table 2 Clinical scores of EAE treated with celecoxib or other non-steroidal anti-inflammatory drugs

	Max. score	Day of onset	Incidence (%)	Cumulative score	Death (%)
Control (CMC)	3.05 ± 0.20	13.10 ± 1.16	100 (10/10)	26.47 ± 5.13	10 (1/10)
Celecoxib	1.02 ± 0.53*	14.30 ± 1.77	90 (9/10)	7.58 ± 6.72*	0 (0/10)
Nimesulid	2.54 ± 0.68	13.50 ± 1.56	100 (10/10)	22.15 ± 4.75	0 (0/10)
Indomethacin	1.70 ± 0.83	13.90 ± 1.93	100 (10/10)	15.21 ± 3.89	100 (10/10)*

Each mouse was immunized with MOG_{35-55} peptide for induction of EAE. The control CMC solution, or 5 μg/g of drugs diluted in CMC, was orally administered via a cannula every other day. Mean ± SEM of the following parameters are shown: maximum score of EAE (Max. score), the days of EAE onset, incidence of paralysed mice among sensitized rats (Incidence), summation of the clinical scores from Day 0 to 30 (Cumulative score) and the incidence of death during EAE (Death). *$P < 0.05$ versus control.

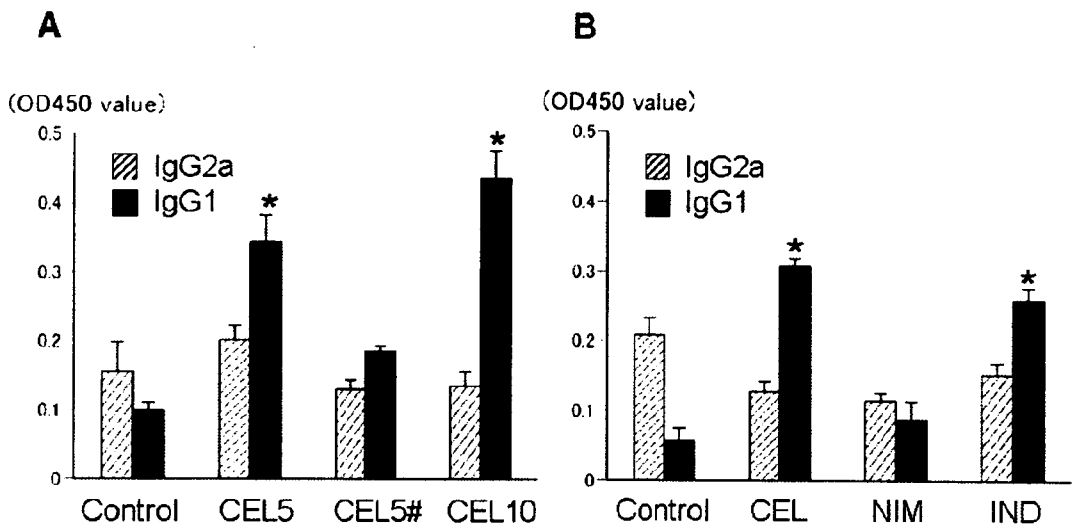

Fig. 3 Analysis of MOG_{35-55} IgG1 and IgG2a in EAE-induced mice. The relative titers of anti-MOG IgG1 and IgG2a in serum samples from individual mice ($n = 10$) on Day 30 after immunization were analysed as indicated in Methods. Data represent mean ± SEM. *$P < 0.05$ versus control. (a) Control = vehicle alone, CEL5 = 5 μg/g of celecoxib, CEL5# = 5 μg/g of celecoxib from Day 8 after the immunization, CEL10 = 10 μg/g of celecoxib. (b) Control = vehicle alone, CEL = celecoxib, NIM = nimesulid, IND = indomethacin.

and Th1 response by celecoxib is mediated by a COX-2-independent pathway (Table 3)

Celecoxib inhibits an infiltration of immune cells into CNS

To characterize the infiltrated cells into CNS, we isolated mononuclear cells from CNS obtained from celecoxib-treated or vehicle-treated mice. Mononuclear cells isolated from the CNS of vehicle-treated mice include $CD3^+$ T cells that comprised >80% of $CD4^+$ cells. In mice treated with celecoxib, the number of infiltrated cells was less than one-seventh compared with vehicle-treated mice (Table 4). In addition, we analysed apoptotic cells from CNS, spleen and draining LNs using annexin-5 staining. There was no difference in the frequency of apoptotic cells in all organs examined from celecoxib-treated and vehicle-treated mice (data not shown). These results suggest that celecoxib inhibits an infiltration of inflammatory cells into the CNS rather than induction of apoptosis of autoreactive T cells.

Celecoxib suppresses the expression of adhesion molecules and a chemokine related to cell infiltration into CNS

For the recruitment of autoreactive T cells into the brain through the blood–brain barrier (BBB), some adhesion molecules such as ICAM-1, VCAM-1 and P-selectin, and chemokines such as MCP-1 are required (Engelhardt *et al.*, 1997; Hofmann *et al.*, 2002). We performed an immunohistostaining of sliced brain sections from mice with EAE using antibodies against adhesion molecules. ICAM-1, VCAM-1 and P-selectin (Fig. 6A, C and E) were expressed on choroid plexus in the brain obtained from EAE-induced mice. In contrast, in brains obtained from celecoxib-treated mice, the expression level of P-selectin and ICAM-1 was lower compared with the control (Fig. 6B, D and F). In addition, we examined the level of MCP-1, which is an important chemokine involved in recruiting autoreactive T cells into the brain. As shown in Table 5, the level of MCP-1 in the serum obtained from

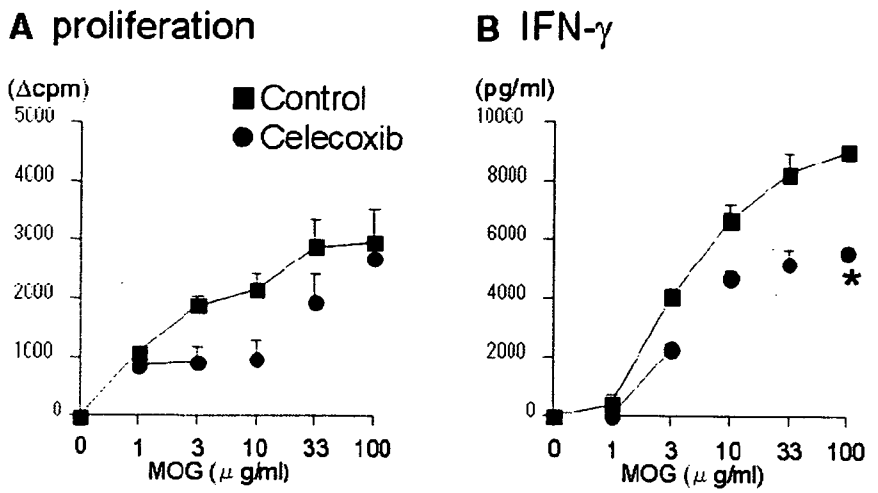

Fig. 4 Comparison of MOG_{35-55}-specific T-cell response after treatment with celecoxib. Popliteal and inguinal LN cells from treated and control animals were incubated in the presence of MOG_{35-55} for 48 h. Proliferative response was determined by the uptake of [^{3}H] thymidine (**A**), and IFN-γ was detected by ELISA (**B**). Representative data of two independent experiments are shown (n = 5 for each group). Error bars represent SEM. *P < 0.05 versus control.

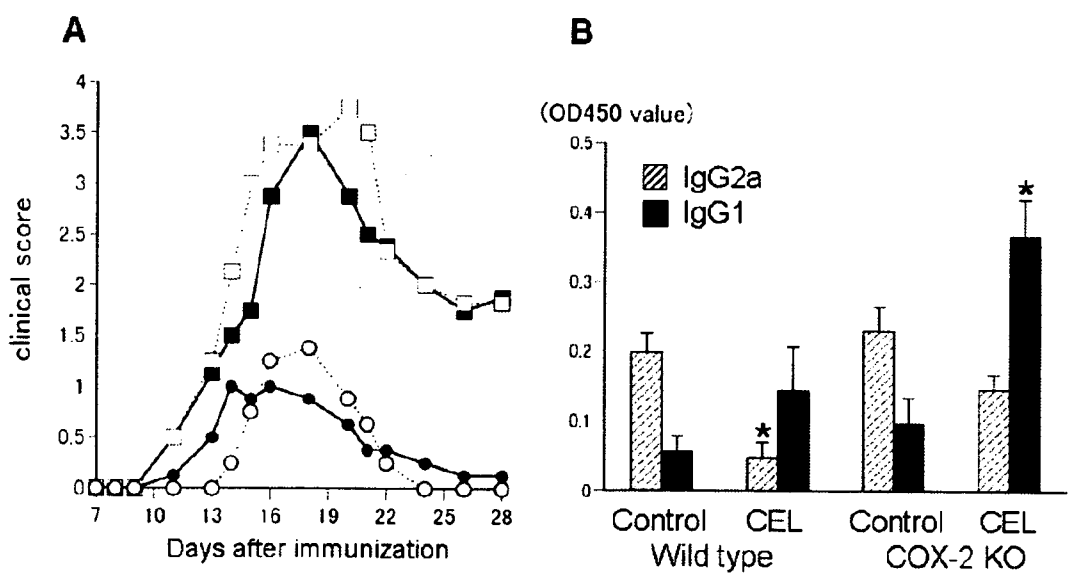

Fig. 5 Effect of celecoxib on actively induced EAE in COX-2-deficient mice. B6 mice and COX-2-deficient mice were immunized with MOG_{35-55} in CFA as described in Material and methods. (**A**) Mice were orally administered celecoxib (5 μg/g) every 2 days starting from the day of the immunization. Statistical analysis is shown in Table 3. Closed squares = vehicle alone for wild-type mice; closed circles = 5 μg/g of celecoxib for wild-type mice, open squares = vehicle alone for COX-2-deficient mice, open circles = 5 μg/g of celecoxib for COX-2-deficient mice. (**B**) The relative titres of anti-MOG IgG1 and IgG2a in serum samples from individual mice on Day 30 after immunization were analysed as indicated in Material and methods. Data represent mean ± SEM. *P < 0.05 versus control. Control = vehicle alone, CEL = celecoxib. One representative experiment of two independent experiments is expressed as mean ± SEM.

celecoxib-treated mice was significantly lower compared with that obtained from vehicle-treated mice. These findings suggested that celecoxib inhibits an infiltration of immune-mediated cells into CNS through the BBB by suppression of P-selectin, ICAM-1 and MCP-1.

Discussion

In the present study, we have demonstrated that a new-generation selective COX-2 inhibitor, celecoxib, strongly inhibited the development of EAE as compared with vehicle treatment or a traditional COX-2 inhibitor, nimesulid. The

Table 3 Clinical scores of EAE in COX-2-deficient mice

Mouse	Treatment	Max. score	Day of onset	Incidence (%)	Cumulative score
Wild-type	CMC	3.54 ± 0.28	12.60 ± 1.15	100 (10/10)	24.85 ± 6.37
	Celecoxib	1.13 ± 0.39*	13.20 ± 1.80	80 (8/10)	6.29 ± 4.02*
COX-2 $^{-/-}$	CMC	3.75 ± 0.44	12.78 ± 1.57	100 (8/8)	29.88 ± 5.62
	Celecoxib	1.46 ± 0.51*	14.13 ± 1.96	87.5 (7/8)	5.39 ± 3.36*

Wild-type and COX-2 $^{-/-}$ mice were immunized with MOG_{35-55} peptide to induce EAE. The control CMC solution, or 5 μg/g of celecoxib diluted in CMC, was administered every other day. Mean ± SEM of the following parameters are shown: maximum score of EAE (Max. score), the days of EAE onset, incidence of paralysed mice among sensitized mice (Incidence) and summation of the clinical scores from Day 0 to 30 (Cumulative score). *$P < 0.05$ versus control.

Table 4 Cell infiltration into the CNS of EAE-induced mice

	Mononuclear cell	$CD3^+$ cell	$CD4^+$ cell	$CD19^+$ cell
EAE mice				
Control (CMC)	667 ± 176	203 ± 69	158 ± 50	6 ± 1
Celecoxib	90 ± 57*	12 ± 8*	9 ± 5*	0 ± 0
Naive mice	20 ± 6	5 ± 2	3 ± 2	1 ± 0

CNS tissues from each group mouse were homogenized on Day 18 after immunization with MOG_{35-55} peptide. Mononuclear cells were isolated by Percoll solution. The cells were stained with cell markers and analysed by flow cytometer. Mean ± SEM of cell number (10^3 cells/mouse) is shown. Representative data of two independent experiments are shown ($n = 5$ for each group). *$P < 0.05$ versus control.

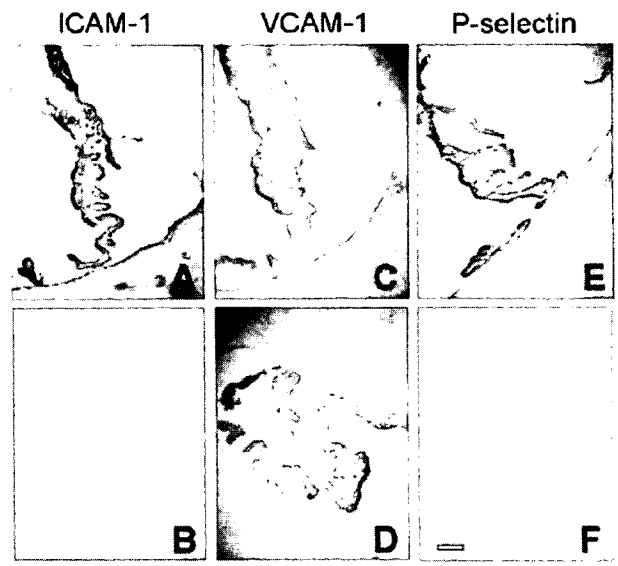

Fig. 6 Immunohistochemical staining with ICAM-1, VCAM-1 and P-selectin of the brain in EAE-induced mice. Brains from EAE mice were removed on Day 14 after immunization as described in Material and methods. Thinly sliced (10 μm) frozen sections of the brain were immunostained with anti-ICAM-1 antibody (**A** and **B**), anti-VCAM-1 antibody (**C** and **D**) and anti-P-selectin antibody (**E** and **F**). Figure shows choroid plexus region. Bar = 100 μm.

inhibitory effect on EAE by celecoxib was also evident in COX-2-deficient mice, indicating that celexoxib suppressed EAE in a COX-2-independent mechanism. In celecoxib-treated mice, MOG-specific Th1 responses were reduced and infiltration of immune cells was significantly inhibited compared with vehicle-treated mice, which were associated with lower expression of ICAM-1 and P-selectin on the choroid plexus in the brain.

Since EAE is an autoimmune inflammatory disease, administering COX-2 inhibitor was expected to inhibit disease as well as other COX inhibitors. Recently, Muthian *et al.* (2006) showed that some COX-2 inhibitors such as NS398 and LM01 suppressed EAE, when administered intraperitoneally every other day. In our study, we could not observe the inhibitory effect of nimesulid on EAE when orally administered every 2 days using the same conditions in which celecoxib exhibited a strong inhibitory effect. The route and timing of administration might be critical to modulate diseases. The inhibitory effect mediated by celecoxib was stronger compared with other COX inhibitors, suggesting that different mechanisms may be occurring in addition to the suppression of production of prostanoids that occurred at sites of disease and inflammation. In fact, COX-2 was not required for the celecoxib-mediated inhibitory effect on EAE. Recent studies have suggested that COX-2-independent pathways may contribute to celecoxib-mediated anti-tumour or anti-arthritic effect through enhanced apoptosis of tumour cells or synovial cells (Kusunoki *et al.*, 2002; Shishodia *et al.*, 2004). In our study, enhancing apoptosis of immune cells was not detected, indicating that different COX-2-independent mechanisms might be important for celecoxib-mediated inhibition of EAE. We observed that celecoxib treatment inhibited Th1 responses of MOG-reactive T cells. In the regulation of Th1/Th2 responses, prostaglandin E2 synthesized by COX has been reported to suppress IL-2 and IFN-γ production by a Th1 clone (Snijdewint *et al.*, 1993). In addition, Meyer *et al.* (2003) reported that administration of COX-2 inhibitor, NS398, increased *Helicobacter*-stimulated IL-12 and IFN-γ production, suggesting that COX-2 inhibition resulted in enhanced Th1 responses. In contrast, celecoxib inhibited Th1 responses of autoreactive T cells. Therefore, this COX-2-independent effect on immune system may be a mechanism to explain why celecoxib suppresses EAE to a greater degree compared with that of other COX-2 inhibitors. Allonza *et al.* (2006) reported that

Table 5 Serum level of MCP-1 in EAE mice after treatment with celecoxib

	Day 0	Day 7	Day 10	Day 14
EAE mice				
Control (CMC) (n = 18)	ND	60.0 ± 21.0	42.6 ± 17.0	ND
Celecoxib (n = 16)	ND	8.5 ± 5.0*	12.9 ± 8.5	ND
Naive mice (n = 10)	ND	ND	ND	ND

B6 mice were immunized with MOG_{35-55} peptide as described in Material and methods. Serum samples from individual mice were collected on Day 0, 7, 10 and 14 after immunization. Serum concentration of MCP-1 was measured by ELISA. Data represent mean ± SEM (pg/ml). ND = not detectable. *$P < 0.05$ versus control.

celecoxib inhibits IL-12 αβ and β2 folding and secretion in association with the increased interaction of IL-12 with calreticulin, an endoplasmic reticulum-resident chaperone in retention of misfolded cargo proteins, while blocking interaction with Erp44. They also demonstrated that an analogue of celecoxib lacking the COX-2 inhibitor activity showed identical effects to that of celecoxib on folding and secretion of IL-12, indicating that the effect is COX-2-independent. Since IL-12 is a key cytokine to provoke Th1 immune response, reduction in MOG-specific Th1 response is consistent with these previous findings.

The infiltration of immune cells in the CNS was significantly inhibited in celecoxib-treated mice. Celecoxib has been reported to reduce expression of P-selectin and ICAM-1 in experimental inflammatory models such as experimental colitis (Cuzzocrea *et al.*, 2001, 2002). In our study, we observed that celecoxib suppressed expression of P-selectin and ICAM-1 in the brain of EAE mice. Since P-selectin and ICAM-1 are the adhesion molecules involved in the recruitment of inflammatory cells into CNS (Engelhardt *et al.*, 1997; Dietrich, 2002; Scott *et al.*, 2004), inhibition of cellular infiltration by celecoxib might be mediated by the downregulation of the expression of adhesion molecules.

Chemokines are also required for recruitment of immune cells into the CNS. MCP-1 is reported to be an essential chemokine in EAE (Hofmann *et al.*, 2002). In the mouse model of atherosclerosis, Wang *et al.* (2005) reported that celecoxib decreased the inflammatory response and hyperplasia following vascular injury through inhibition of MCP-1 induction. We detected a decreased level of MCP-1 in the serum in celecoxib-treated mice on EAE. The suppression of MCP-1 by celecoxib might also contribute to the reduction of infiltrating cells into the CNS.

In conclusion, celecoxib has a potent therapeutic potential for EAE by inducing a Th2 bias and suppressing infiltration of inflammatory cells into the CNS through a COX-2-independent mechanism. Further analysis of celecoxib-mediated suppression of EAE will help drug development for multiple sclerosis. Celecoxib is hoped to be a new choice of the treatment of multiple sclerosis.

Acknowledgement

This study was supported by the Japan Research Foundation for Clinical Pharmacology.

References

Alloza I, Baxter A, Chen Q, Matthiesen R, Vanderbroeck K. Celecoxib inhibits interleukin-12 αβ and β2 folding and secretion by a novel COX2-independent mechanism involving chaperones of the endoplasmic reticulum. Mol Pharm 2006; 69: 1579–87.

Arico S, Pattingre S, Bauvy C, Gane P, Barbat A, Codogno P, et al. Celecoxib induces apoptosis by inhibiting 3-phosphoinositide-dependent protein kinase-1 activity in the human colon cancer HT-29 cell line. J Biol Chem 2002; 277: 27613–21.

Cuzzocrea S, Mazzon E, Serraino I, Dugo L, Centorrino T, Ciccolo A, et al. Celecoxib, a selective cyclo-oxygenase-2 inhibitor reduces the severity of experimental colitis induced by dinitrobenzene sulfonic acid in rats. Eur J Pharmacol 2001; 431: 91–102.

Cuzzocrea S, Mazzon E, Sautebin L, Dugo L, Serraino I, De Sarro A, et al. Protective effects of celecoxib on lung injury and red blood cells modification induced by carrageenan in the rat. Biochem Pharmacol 2002; 63: 785–95.

Deininger MH, Schluesener HJ. Cyclooxygenases-1 and -2 are differentially localized to microglia and endothelium in rat EAE and glioma. J Neuroimmunol 1999; 95: 202–8.

Dietrich JB. The adhesion molecule ICAM-1 and its regulation in relation with the blood-brain barrier. J Neuroimmunol 2002; 128: 58–68.

Engelhardt B, Vestweber D, Hallmann R, Schulz M. E- and P-selectin are not involved in the recruitment of inflammatory cells across the blood-brain barrier in experimental autoimmune encephalomyelitis. Blood 1997; 90: 4459–72.

Grosch S, Tegeder I, Niederberger E, Brautigam L, Geisslinger G. COX-2 independent induction of cell cycle arrest and apoptosis in colon cancer cells by the selective COX-2 inhibitor celecoxib. FASEB J 2001; 15: 2742–4.

Hofmann N, Lachnit N, Streppel M, Witter B, Neiss WF, Guntinas-Lichius O, et al. Increased expression of ICAM-1, VCAM-1, MCP-1, and MIP-1 alpha by spinal perivascular macrophages during experimental allergic encephalomyelitis in rats. BMC Immunol 2002; 6: 11.

Hsu AL, Ching TT, Wang DS, Song X, Rangnekar VM, Chen CS. The cyclooxygenase-2 inhibitor celecoxib induces apoptosis by blocking Akt activation in human prostate cancer cells independently of Bcl-2. J Biol Chem 2000; 275: 11397–403.

Krakowski ML, Owens T. The central nervous system environment controls effector CD4+ T cell cytokine profile in experimental allergic encephalomyelitis. Eur J Immunol 1997; 27: 2840–7.

Kumar V, Aziz F, Sercarz E, Miller A. Regulatory T cells specific for the same framework 3 region of the Vb8.2 chain are involved in the control of collagen II-induced arthritis and experimental autoimmune encephalomyelitis. J Exp Med 1997; 185: 1725–33.

Kusunoki N, Yamazaki R, Kawai S. Induction of apoptosis in rheumatoid synovial fibroblasts by celecoxib, but not by other selective cyclooxygenase 2 inhibitors. Arthritis Rheum 2002; 46: 3159–67.

Liu X, Yue P, Zhou Z, Khuri FR, Sun SY. Death receptor regulation and celecoxib-induced apoptosis in human lung cancer cells. J Natl Cancer Inst 2004; 96: 1769–80.

Meyer F, Ramanujam KS, Gobert AP, James SP, Wilson KT. Cutting edge: cyclooxygenase-2 activation suppresses Th1 polarization in response to Helicobacter pylori. J Immunol 2003; 171: 3913–7.

Miyamoto K, Oka N, Kawasaki T, Satoi H, Akiguchi I, Kimura J. The effect of cyclooxygenase-2 inhibitor on experimental allergic neuritis. Neuroreport 1998; 9: 2331–4.

Miyamoto K, Oka N, Kawasaki T, Satoi H, Matsuo A, Akiguchi I. The action mechanism of cyclooxygenase-2 inhibitor for treatment of experimental allergic neuritis. Muscle Nerve 1999; 22: 1704–9.

Miyamoto K, Oka N, Kawasaki T, Miyake S, Yamamura T, Akiguchi I. New cyclooxygenase-2 inhibitor for treatment of experimental autoimmune neuritis. Muscle Nerve 2002; 25: 280–2.

Muthian G, Raikwar HP, Johnson C, Rajasingh J, Kalgutkar A, Marnett LJ, et al. COX-2 inhibitors modulate IL-12 signaling through JAK-STAT pathway leading to Th1 response in experimental allergic encephalomyelitis. J Clin Immunol 2006; 26: 73–85.

Nakatsuji S, Terada N, Yoshimura T, Horie Y, Furukawa M. Effects of nimesulide, a preferential cyclooxygenase-2 inhibitor, on carrageenan-induced pleurisy and stress-induced gastric lesions in rats. Prostaglandins 1996; 55: 395–402.

Nicholson LB, Kuchroo VK. Manipulation of the Th1/Th2 balance in autoimmune disease. Curr Opin Immunol 1996; 8: 837–42.

Penning TD, Talley JJ, Bertenshaw SR, Carter JS, Collins PW, Docter S, et al. Synthesis and biological evaluation of the 1,5-diarylpyrazole class of cyclooxygenase-2 inhibitors: identification of 4-[5-(4-methylphenyl)-3-(trifluoromethyl)-1H-pyrazol-1-yl]benzene sulfonamide (SC-58635, celecoxib). J Med Chem 1997; 40: 1347–65.

Prosiegel M, Neu I, Mallinger J, Wildfeuer A, Mehlber L, Vogl S, et al. Suppression of experimental autoimmune encephalomyelitis by dual cyclooxygenase and 5-lipoxygenase inhibition. Acta Neurol Scand 1989; 79: 223–6.

Scott GS, Kean RB, Fabis MJ, Mikheeva T, Brimer CM, Phares TW, et al. ICAM-1 upregulation in the spinal cords of PLSJL mice with experimental allergic encephalomyelitis is dependent upon TNF-alpha production triggered by the loss of blood-brain barrier integrity. J Neuroimmunol 2004; 155: 32–42.

Shishodia S, Koul D, Aggarwal BB. Cyclooxygenase (COX)-2 inhibitor celecoxib abrogates TNF-induced NF-kappa B activation through inhibition of activation of I kappa B alpha kinase and Akt in human non-small cell lung carcinoma: correlation with suppression of COX-2 synthesis. J Immunol 2004; 173: 2011–22.

Simmons RD, Hugh AR, Willenborg DO, Cowden WB. Suppression of active but not passive autoimmune encephalomyelitis by dual cyclo-oxygenase and 5-lipoxygenase inhibition. Acta Neurol Scand 1992; 85: 197–9.

Snijdewint F, Kalinski P, Wierenga E, Bos J, Kapasenberg M. Prostaglandin E2 differentially modulate cytokine secretion profiles of human T helper lymphocytes. J Immunol 1993; 150: 5321.

Vane JR, Mitchell JA, Appleton I, Tomlinson A, Bishop-Bailey D, Croxtall J, et al. Inducible isoforms of cyclooxygenase and nitric oxide synthase in inflammation. Proc Natl Acad Sci USA 1994; 91: 2046–50.

Wang K, Tarakji K, Zhou Z, Zhang M, Forudi F, Zhou X, et al. Celecoxib, a selective cyclooxygenase-2 inhibitor, decreases monocyte chemoattractant protein-1 expression and neointimal hyperplasia in the rabbit atherosclerotic balloon injury model. J Cardiovasc Pharmacol 2005; 45: 61–7.

Warner TD, Mitchell JA. Cyclooxygenases: new forms, new inhibitors, and lessons from the clinic. FASEB J 2004; 18: 790–804.

Weber F, Meyermann R, Hempel K. Experimental allergic encephalomyelitis-prophylactic and therapeutic treatment with the cyclooxygenase inhibitor piroxicam (Feldene). Int Arch Allergy Appl Immunol 1991; 95: 136–41.

Xie WL, Chipman JG, Robertson DL, Erikson RL, Simmons DL. Expression of a mitogen-responsive gene encoding prostaglandin synthase is regulated by mRNA splicing. Proc Natl Acad Sci USA 1991; 88: 2692–6.

Zhang B, Yamamura T, Kondo T, Fujiwara M, Tabira T. Regulation of experimental autoimmune encephalomyelitis by natural killer (NK) cells. J Exp Med 1997; 186: 1677–87.

nature immunology

Invariant V_α19i T cells regulate autoimmune inflammation

J Ludovic Croxford[1], Sachiko Miyake[1], Yi-Ying Huang[2], Michio Shimamura[2] & Takashi Yamamura[1]

T cells expressing an invariant V_α19-J_α33 T cell receptor α-chain (V_α19i TCR) are restricted by the nonpolymorphic major histocompatibility complex class Ib molecule MR1. Whether V_α19i T cells are involved in autoimmunity is not understood. Here we demonstrate that T cells expressing the V_α19i TCR transgene inhibited the induction and progression of experimental autoimmune encephalomyelitis (EAE), a mouse model of multiple sclerosis. Similarly, EAE was exacerbated in MR1-deficient mice, which lack V_α19i T cells. EAE suppression was accompanied by reduced production of inflammatory mediators and increased secretion of interleukin 10. Interleukin 10 production occurred at least in part through interactions between B cells and V_α19i T cells mediated by the ICOS costimulatory molecule. These results suggest an immunoregulatory function for V_α19i T cells.

Two distinct mouse T cell subsets express invariant TCRα chains: V_α14-J_α18 (V_α14i; ref. 1) and V_α19-J_α33 (V_α19i; ref. 2). Although conventional T cells recognize peptide antigens presented by polymorphic major histocompatibility complex class Ia molecules, V_α14i 'invariant' T cell populations recognize nonpeptide antigens[3,4] presented in the context of the nonpolymorphic major histocompatibility complex class Ib molecule CD1d. MR1 may be able to present glycolipids *in vitro* to V_α19i T cells[5], but the identity or type of endogenous ligand recognized by V_α19i T cells *in vivo* is unknown. However, antigen recognition is essential for the development of T cells expressing V_α14i and V_α19i TCR chains, as these subsets are absent from *Cd1d1*$^{-/-}$ and *Mr1*$^{-/-}$ mice, respectively[6,7]. Similar invariant T cell subsets are present in humans[8,9]. Many of these cells also express natural killer (NK) cell markers on their surface (such as mouse NK1.1). Consequently, CD1d-restricted invariant T cells have traditionally been referred to as 'NKT cells' (V_α14i NKT cells)[10].

Transgenic overexpression of the V_α14i TCR chain protects against the development of mouse models of type I diabetes[11] and multiple sclerosis[12], suggesting that V_α14i NKT cells may be involved in regulating autoimmunity. In addition, susceptibility to type I diabetes is linked to quantitative and functional deficiencies in V_α14i NKT cells[13]. Mechanistic studies suggest that V_α14i NKT cells may down regulate autoimmunity by increasing the production of T helper type 2 (T_H2) cytokines[14–19]. However, in other conditions, NKT cells may promote the exacerbation of autoimmune disease. V_α14i NKT cell–deficient mice show ameliorated arthritis compared with that of their wild-type counterparts[18,20,21].

The immune function of MR1-restricted invariant T cells remains less clear than that of CD1d-restricted lymphocytes. MR1-restricted invariant T cells were first identified among human peripheral blood $CD4^-CD8^-$ T cells as a clonally expanded population expressing an invariant V_α7.2-J_α33 TCR chain (V_α7.2i T cells)[22]. Subsequent studies identified clonally expanded T cells expressing the highly homologous invariant V_α19-J_α33 TCR chain in mice and cattle[9]. V_α19i T cell development has been found to depend on the nonpolymorphic major histocompatibility complex class Ib molecule MR1 and on the presence of B cells[7]. The V_α19i TCR is uniquely overexpressed in the gut lamina propria and V_α19i T cell development depends on the presence of commensal gut flora, indicating potential involvement of these cells in gut immunity[2,7]. As MR1 molecules are thought to be retained in the endoplasmic reticulum, intestinal flora might provide exogenous ligands for the V_α19i TCR, or a cellular 'stress' signal, that enables transit of MR1 from the endoplasmic reticulum to the cell surface[2,7].

Human V_α7.2i T cells[2] but not mouse gut V_α19i T cells express NKT cell markers[7]. In contrast, the V_α19i TCR is expressed by most T cell hybridomas derived from liver $NK1.1^+$ T cells from *Cd1d1*$^{-/-}$ mice[23]. Furthermore, 25–50% of V_α19i cells from V_α19i transgenic mice on a *Tcra*$^{-/-}$ background express NK1.1 (ref. 24). Those divergent results regarding NK1.1 expression remain unclear, but may be due to differences among mouse genetic backgrounds. Alternatively, as with CD1d-restricted T cells, a subpopulation of MR1-restricted T cells may lack NK1.1 expression. Based on their predominant distribution in the gut, MR1-restricted T cells are often referred to as 'mucosal-associated invariant T cells'[2,7]. To avoid confusion, we subsequently use the term 'V_α19i T cells' to describe V_α19i T cells expressing NK1.1.

The V_α7.2i TCR is over-represented in central nervous system (CNS) lesions from multiple sclerosis autopsy samples[25], whereas the V_α24i TCR is mostly absent[26]. Those findings led us to speculate that MR1-restricted T cells may 'preferentially' migrate to CNS lesions,

[1]Department of Immunology, National Institute of Neuroscience, National Centre of Neurology and Psychiatry, Tokyo 187-8502, Japan. [2]Developmental Immunology Unit, Mitsubishi Kagaku Institute of Life Sciences, Tokyo 194-8511, Japan. Correspondence should be addressed to T.Y. (yamamura@ncnp.go.jp).

Received 26 May; accepted 5 July; published online 30 July 2006; doi:10.1038/ni1370

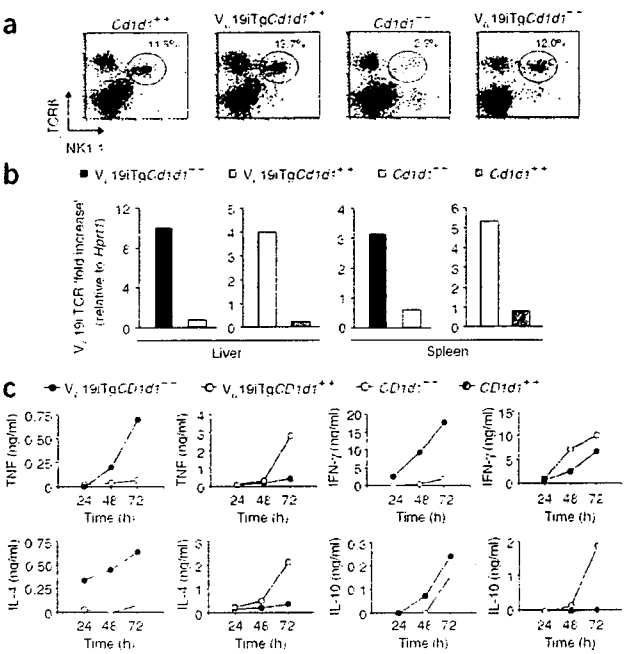

Figure 1 Characterization of NK1.1$^+$ T cells from V_α19iTg mice. (**a**) Flow cytometry of liver NK1.1$^+$ T cells 48 h after anti-asialo-GM1-mediated depletion of NK cells (mouse genotypes, above plots). Numbers above gated regions indicate the percentage of NK1.1$^+$TCRβ$^+$ cells. (**b**) Real-time RT-PCR of V_α19i TCR mRNA expression in liver or spleen NK1.1$^+$ T cells (mouse genotypes, key). Data are presented as 'fold increase' over expression of *Hprt1*. (**c**) Cytokines in the supernatants of sorted liver NK1.1$^+$ T cells (mouse genotypes, key) stimulated by immobilized anti-CD3 *in vitro*, measured at 24, 48 and 72 h after stimulation. Data are representative of two separate experiments (**a**,**b**) or the mean of two replicate values from two separate experiments (**c**).

where they regulate CNS inflammation. We designed this study to address the function of MR1-restricted T cells in experimental autoimmune encephalomyelitis (EAE)[14,17], a mouse model of multiple sclerosis. Here we report that over-representation of V_α19i T cells decreased the severity of EAE, whereas depletion of V_α19i T cells exacerbated EAE. Furthermore, V_α19i T cells exerted an influence on the phenotype and functions of autoimmune T cells in the draining lymph nodes and spleens of mice. In particular, over-representation of V_α19i T cells reduced the production of proinflammatory cytokines and increased the production of interleukin 10 (IL-10), which may account for V_α19i T cell–mediated suppression of autoimmune disease. Finally, interactions between V_α19i T cells and B cells mediated by the ICOS costimulatory molecule increased B cell IL-10 production and may therefore represent a mechanism by which V_α19i T cells regulate inflammation.

RESULTS

Characterization of transgenic V_α19i T cells

An antibody specific for the V_α19i TCR chain does not exist, and wild-type mice have very few MR1-restricted V_α19i T cells. Therefore, to circumvent those experimental hurdles and to evaluate the function of V_α19i T cells *in vivo*, we used V_α19i TCR–transgenic (V_α19iTg) mice[5], which were originally generated by injection into C57BL/6 mouse oocytes of a transgenic construct encoding a V_α19-J_α33 TCR construct driven by the endogenous *Tcra* promoter. We crossed the transgenic line with *Cd1d1*$^{+/+}$ and *Cd1d1*$^{-/-}$ C57BL/6 mice for seven to nine generations. First we compared numbers of liver NK1.1$^+$ T cells present in *Cd1d1*$^{+/+}$, *Cd1d1*$^{-/-}$, V_α19iTg*Cd1d1*$^{+/+}$ and V_α19iTg*Cd1d1*$^{-/-}$ mice (**Fig. 1a**). TCRβ$^+$NK1.1$^+$ T cells comprised 11.5% of total liver lymphocytes in *Cd1d1*$^{+/+}$ mice but only 2.3% of total liver lymphocytes in *Cd1d1*$^{-/-}$ mice. Therefore, most (about 80%) of NK1.1$^+$ T cells in *Cd1d1*$^{+/+}$ mice corresponded to CD1d-restricted V_α14i NKT cells, whereas about 20% were probably MR1 restricted[23]. Notably, V_α19iTg*Cd1d1*$^{-/-}$ mice had many NK1.1$^+$ T cells (12.0%), indicating that overexpression of the V_α19i TCR in *Cd1d1*$^{-/-}$ mice compensated for the reduction in NK1.1$^+$ T cells caused by CD1d deficiency. In contrast, the number of NK1.1$^+$ T cells was only slightly higher in V_α19iTg*Cd1d1*$^{+/+}$ mice, which had normal numbers of V_α14i NKT cells. To confirm that the NK1.1$^+$ T cell population in V_α19iTg mice was enriched in cells expressing the V_α19i TCR chain, we measured V_α19i mRNA transcripts in NK1.1$^+$ liver cells and splenocytes by real-time RT-PCR (**Fig. 1b**). V_α19i mRNA expression was much greater in liver and splenic NK1.1$^+$ T cell populations from V_α19iTg*Cd1d1*$^{+/+}$ or V_α19iTg*Cd1d1*$^{-/-}$ mice than in those from nontransgenic littermates (**Fig. 1b**). In V_α19i T cells, the V_α19i TCR chain 'preferentially' associates with TCRβ chains containing V_β8 or V_β6 segments[24]. Approximately 60–70% of liver NKT cells from V_α19iTg*Cd1d1*$^{-/-}$ or V_α19iTg*Tcra*$^{-/-}$ mice expressed either V_β8 or V_β6, compared with 30–40% of conventional T cells in the same mice (unpublished observations). These observations collectively demonstrate that NK1.1$^+$ T cell populations in V_α19iTg mice are highly enriched in cells expressing V_α19-J_α33 TCR chains and V_β6 or V_β8 TCR chains. Next we compared the ability of NK1.1$^+$ T cells from V_α19iTg and nontransgenic mice to produce immunosuppressive cytokines. To obtain V_α19i T cells, we depleted V_α19iTg*Cd1d1*$^{-/-}$ mice of NK cells by injecting antibody to

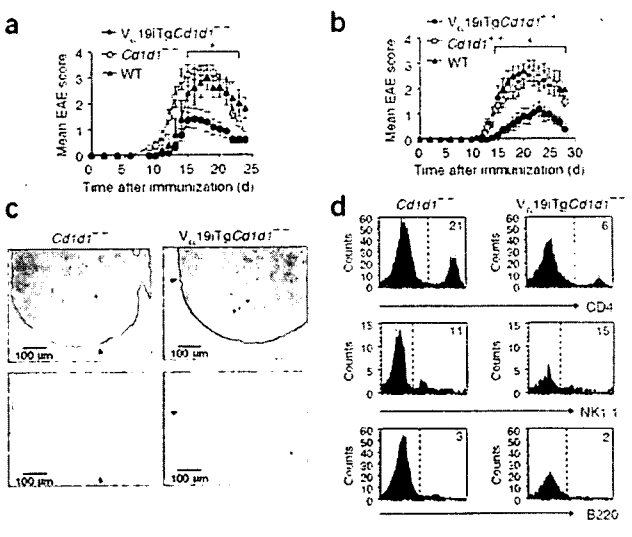

Figure 2 V_α19i T cells in EAE. (**a**,**b**) Clinical EAE scores of mice immunized with MOG(35–55). WT, wild-type. Data represent mean score ± s.e.m. from three independent experiments (n = 10–22 mice). (**c**) Monocyte infiltration and demyelination (arrowheads) of the lumbar spinal cord during EAE (day 15). (**d**) Quantification of spinal cord cellular infiltrates by flow cytometry. Areas to the right of dashed lines indicate positive cellular staining; numbers in histograms indicate percentage of CD4$^+$, NK1.1$^+$ (gated on CD3$^+$) or B220$^+$ cells. *, $P < 0.05$ (Mann-Whitney U-test). Data are representative of three separate experiments.

Table 1 V_α19i T cells in EAE

Group	Mice with EAE	Group score	EAE score	Day of onset
Wild-type	10 of 10	3.3 ± 0.3	3.3 ± 0.3	13.6 ± 0.7
Cd1d1$^{-/-}$	18 of 18	3.4 ± 0.2	3.4 ± 0.2	11.7 ± 0.5
V_α19iTg*Cd1d1*$^{-/-}$	13 of 22	1.3 ± 0.3***	2.2 ± 0.2**	14.3 ± 0.6**
Wild-type	7 of 7	3.6 ± 0.2	3.6 ± 0.2	13.6 ± 0.5
Cd1d1$^{+/+}$	11 of 11	3.3 ± 0.4	3.3 ± 0.4	14.8 ± 0.7
V_α19iTg*Cd1d1*$^{+/+}$	9 of 13	1.3 ± 0.3**	1.9 ± 0.4*	18.6 ± 1.2**
NK1.1$^-$ AdTx	10 of 10	3.6 ± 0.3	3.6 ± 0.3	11.6 ± 0.5
V_α19i AdTx	8 of 10	2.2 ± 0.4*	2.8 ± 0.3	15.8 ± 0.6***
Mr1$^{+/+}$	10 of 10	3.0 ± 0.2	3.0 ± 0.2	13.9 ± 0.5
Mr1$^{-/-}$	8 of 8	4.0 ± 0.0**	4.0 ± 0.0*	11.5 ± 0.5***

Clinical outcome of mice immunized with MOG(35–55) to induce EAE. Data represent number of mice with EAE (of total mice in group); mean group EAE score (± s.e.m.); mean EAE score excluding mice without evidence of EAE (± s.e.m.); and mean day of onset (± s.e.m.). In one experiment, mice received adoptive transfer (AdTx) of V_α19i T cells or NK1.1$^-$ cells as a control. *, $P < 0.05$, **, $P < 0.01$, and ***, $P < 0.001$, compared with control groups (Mann-Whitney U nonparametric test).

asialo-GM1 (anti-asialo-GM1). We then sorted NK1.1$^+$ cells from the liver. When activated by plate-bound anti-CD3, NK1.1$^+$ T cells from *Cd1d1*$^{+/+}$ mice secreted more interferon-γ (IFN-γ), tumor necrosis factor (TNF) and interleukin 4 (IL-4) than did those from *Cd1d1*$^{-/-}$ mice, confirming that CD1d-restricted T cells are a chief source of cytokines (**Fig. 1c**). However, NK1.1$^+$ T cells from V_α19iTg mice secreted more T_H1 cytokines (IFN-γ and TNF) and T_H2 cytokines (IL-4 and IL-10) than did NK1.1$^+$ T cells from nontransgenic littermates (**Fig. 1c**). During subsequent experiments, we used V_α19iTg*Cd1d1*$^{-/-}$ mice as a source of V_α19i T cells.

V_α19i T cells in EAE

To determine if an abundance of V_α19i T cells could modulate autoimmune disease, we analyzed the development and progression of EAE in V_α19iTg mice. We induced EAE by immunizing mice with a peptide of amino acids 35–55 of myelin oligodendrocyte glycoprotein (MOG(35–55)). The presence of the V_α19i transgene suppressed the development and progression of EAE, regardless of whether CD1d-restricted NKT cells were present (**Fig. 2a,b** and **Table 1**). The onset of EAE was delayed in V_α19iTg mice, and the incidence and severity of clinical EAE was reduced.

Histological examination of the lumbar (L3) region of the spinal cord 15 d after EAE induction showed less monocyte infiltration and demyelination (assessed by luxol fast blue staining) in V_α19iTg*Cd1d1*$^{-/-}$ mice than in *Cd1d1*$^{-/-}$ mice (**Fig. 2c**). In agreement with the histology, spinal cords of *Cd1d1*$^{-/-}$ mice contained three times more infiltrating cells than did those from V_α19iTg*Cd1d1*$^{-/-}$ mice (0.09×10^6 and 0.03×10^6 cells respectively, pooled from three mice). Flow cytometry showed fewer CD4$^+$ T cells infiltrating the CNS at an active stage of EAE (day 15) in V_α19iTg*Cd1d1*$^{-/-}$ mice (6%) than in nontransgenic littermates (21%; **Fig. 2d**). Moreover, 11% and 15% of CNS-infiltrating CD3$^+$ T cells expressed NK1.1$^+$ in *Cd1d1*$^{-/-}$ and V_α19iTg*Cd1d1*$^{-/-}$ mice, respectively, and NK1.1$^+$ T cells comprised between 1% and 2% of total CNS-infiltrating cells (**Fig. 2d**). Also, few B cells trafficked into the CNS during EAE (3% and 2% in *Cd1d1*$^{-/-}$ and V_α19iTg*Cd1d1*$^{-/-}$, respectively, **Fig. 2d**). To determine potential mechanisms of reduced CNS infiltration, we analyzed the expression of chemokine receptors and adhesion molecules necessary for T cell migration into the CNS. TCRβ$^+$CD4$^+$ T cells isolated from the CNS, lymph nodes and spleens of V_α19iTg*Cd1d1*$^{-/-}$ and *Cd1d1*$^{-/-}$ mice on day 18 after EAE induction had similar surface expression of CCR1 and CCR2 (data not shown). However, V_α19iTg*Cd1d1*$^{-/-}$ mice had fewer CD44$^+$ and CD49d$^+$ TCRβ$^+$ splenocytes than did *Cd1d1*$^{-/-}$ mice (**Supplementary Fig. 1** online).

Next we examined recall responses of MOG(35–55)-primed T cells by *ex vivo* rechallenge with MOG(35–55) on day 10 after disease induction. Compared with nontransgenic cells, lymph node cells from MOG(35–55)-primed V_α19iTg*Cd1d1*$^{-/-}$ mice produced less pro-inflammatory cytokines (IFN-γ, TNF, IL-2 and IL-17) and more immunosuppressive IL-10 ($P < 0.05$; **Fig. 3a**). IL-4 and IL-5 were below the limits of analysis detection (less than 5 pg/ml).

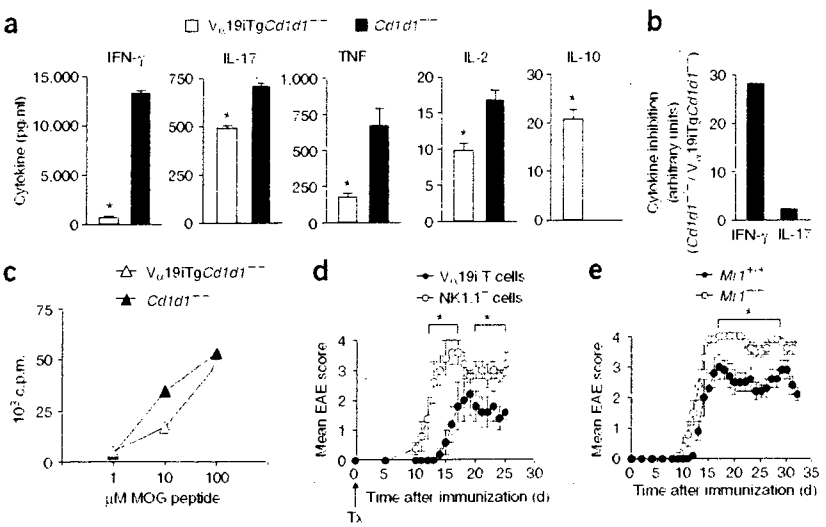

Figure 3 Inhibition of EAE is associated with decreased T_H1 cytokine production. (**a**) Cytometric bead assay of cytokines in the supernatants of MOG-specific lymph node cells (1×10^6) isolated from mice on day 10 after EAE induction and rechallenged with 100 μM MOG(35–55) *in vitro*, measured 72 h after rechallenge. Data represent the mean ± s.e.m. of duplicate samples from three separate experiments. *, $P < 0.05$ (two-tailed Student's *t*-test). (**b**) Inhibition of IFN-γ or IL-17 in V_α19iTg*Cd1d1*$^{-/-}$ mice versus *Cd1d1*$^{-/-}$ mice from **a**, presented as 'fold inhibition' of cytokine, calculated as the cytokine concentration from *Cd1d1*$^{-/-}$ mice divided by the cytokine concentration from V_α19iTg*Cd1d1*$^{-/-}$ mice. (**c**) T cell proliferation of cell preparations identical to those in **a** from lymph nodes (mouse genotypes, key) rechallenged for 72 h with varying doses of MOG(35–55), assessed by [^{3}H]thymidine incorporation. Data represent the mean of triplicate samples from three separate experiments. (**d**) Clinical EAE scores of wild-type nontransgenic mice ($n = 10$) that received 1×10^6 sorted V_α19i T cells or an equal number of NK1.1$^-$ TCRβ$^+$ liver cells from V_α19iTg*Cd1d1*$^{-/-}$ mice on the day of immunization with MOG(35–55). Tx indicates the day of adoptive transfer of cells. (**e**) Clinical EAE scores of *Mr1*$^{-/-}$ and *Mr1*$^{+/+}$ mice ($n = 8$–10) immunized with MOG(35–55). Data are representative of triplicate samples from three separate experiments.

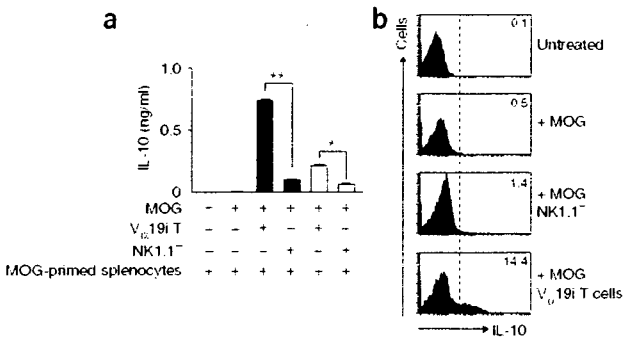

Figure 4 Interactions of V_γ19i T cells and splenocytes induce IL-10. (**a**) Cytometric bead assay of IL-10 in the supernatants of liver V_γ19i T cells from naive V_α19iTg*Cd1d1*$^{-/-}$ mice, cultured for 72 h with MOG(35–55)-specific splenocytes and MOG(35–55) (filled bars). In some cases, V_γ19i T cells were separated from splenocytes by transwell inserts (open bars). Controls received NK1.1$^-$ liver cells from V_α19iTg*Cd1d1*$^{-/-}$ mice. Data represent ± s.e.m. from duplicate samples from three independent experiments. *, $P < 0.01$, and **, $P < 0.001$, compared with control (two-tailed Student's *t*-test). (**b**) Intracellular flow cytometry of IL-10 production by total cells from **a**. Areas to the right of dashed lines indicate positive cellular staining; numbers in histograms indicate percentages of IL-10-producing cells. Data are representative of three separate experiments.

IFN-γ secretion was more susceptible to the inhibitory effects of V_α19i T cells than was IL-17 (**Fig. 3b**). Splenocytes acted like lymph node cells (data not shown).

Overexpression of the V_α19i TCR might compromise the ability of conventional T cells to recognize myelin-derived peptides. However, the proliferative responses of MOG(35–55)-reactive T cells were not lower in V_α19iTg*Cd1d1*$^{-/-}$ mice, despite the inhibition of T_H1 cytokine production (**Fig. 3c**). Therefore, it is unlikely that the degree of EAE suppression seen in V_α19iTg*Cd1d1*$^{-/-}$ mice was the result of alterations in the MOG(35–55)-specific T cell repertoire. However, to exclude that possibility, we did adoptive transfer experiments. We transferred 1×10^6 V_α19i T cells isolated from V_α19iTg*Cd1d1*$^{-/-}$ mice into nontransgenic mice on the day of EAE induction. Mice that received TCRβ$^+$ T cells were significantly protected from EAE (**Fig. 3d**) and the onset of clinical disease was significantly delayed (**Table 1**) compared with that of mice that received V_α19i$^-$ NK1.1$^-$ T cells.

Next we sought to determine if V_α19i T cell deficiency could also influence clinical EAE. As no V_α19i-specific TCR antibody is available to deplete mice of V_α19i T cells *in vivo*, we used *Mr1*$^{-/-}$ mice, which lack V_α19i T cells[7]. As wild-type nontransgenic mice have about four times more V_α14i NKT cells than V_α19i T cells and *Cd1d1*$^{-/-}$mice did not show protection from EAE (**Fig. 2a**), we sought to determine whether the deletion of small numbers of MR1-restricted T cells could alter the clinical course of EAE. Compared with wild-type nontransgenic controls, *Mr1*$^{-/-}$ mice showed a significantly more severe form of EAE with an earlier onset ($P < 0.05$; **Fig. 3e** and **Table 1**). Furthermore, T cells from *Mr1*$^{-/-}$ mice proliferated more and produced more T_H1 cytokines and less IL-10 (data not shown). These experiments collectively suggest that V_α19i T cells have a regulatory function in a T_H1-mediated autoimmune disease.

V_α19i T cells induce B cell IL-10 production

MOG(35–55)-primed V_α19iTg lymph node cells and splenocytes secreted IL-10, which potently inhibits EAE[27–30] (**Fig. 3a**). Therefore, we sought to determine whether an increase in V_α19i T cells augmented general IL-10 production. To address that, we developed a mixed-lymphocyte assay in which we cultured NK1.1$^+$ or NK1.1$^-$ T cells from V_α19iTg*Cd1d1*$^{-/-}$ mice together with MOG(35–55)-primed nontransgenic splenocytes (**Fig. 4a**). Neither NK1.1$^+$ or NK1.1$^-$ T cells inhibited the proliferation of MOG(35–55)-primed splenic T cells restimulated with MOG(35–55) (data not shown). Cytokine analysis showed that the coculture supernatant contained considerable IL-10 (after stimulation with MOG(35–55)) in the presence of NK1.1$^+$ but not NK1.1$^-$ T cells from V_α19iTg*Cd1d1*$^{-/-}$ mice (**Fig. 4a**). NK1.1$^+$ T cells from V_α19iTg*Cd1d1*$^{-/-}$ mice induced IL-10 production even in the absence of MOG(35–55) ($P < 0.05$; **Supplementary Fig. 2** online). However, IL-10 secretion was significantly enhanced in the presence of exogenous MOG(35–55) ($P < 0.01$; **Supplementary Fig. 2**). Intracellular cytokine analysis confirmed that IL-10 production was induced by the addition of NK1.1$^+$ but not NK1.1$^-$ T cells from V_α19iTg*Cd1d1*$^{-/-}$ mice (**Fig. 4b**). However, in the presence of transwell inserts, IL-10 production was inhibited, indicating that V_α19i T cell–mediated IL-10 production depends mainly on cell-cell contact (**Fig. 4a**). IL-4 and IL-5 were below the limit of detection (less than 5 pg/ml), and IFN-γ and TNF were slightly upregulated in the presence of V_α19i T cells (data not shown).

To determine which cells produced IL-10, in the same coculture experiment we analyzed IL-10 production by CD19$^+$, CD4$^+$, CD8$^+$,

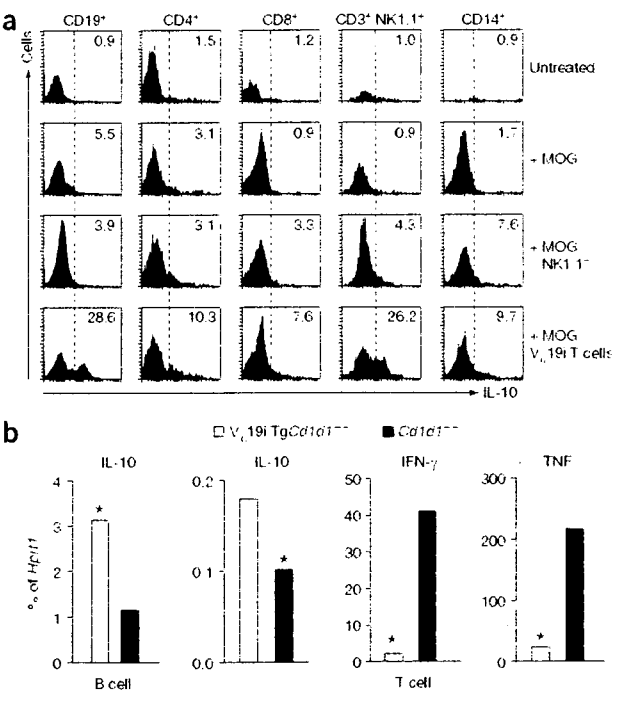

Figure 5 V_α19i T cells induce B cells to secrete IL-10. (**a**) Intracellular flow cytometry of IL-10 production by liver V_α19i T cells from naive V_γ19iTg*Cd1d1*$^{-/-}$ mice, cultured for 72 h with MOG(35–55)-specific splenocytes and MOG(35–55). Areas to the right of dashed lines indicate positive cellular staining; numbers in histograms indicate percentage of IL-10-producing cells expressing various surface markers (above plots). Data are representative of two separate experiments. (**b**) Real-time RT-PCR of the expression of transcripts encoding various cytokines (above graphs) by splenic CD19$^+$ B cells or CD4$^+$ T cells sorted from mice with EAE. Data are expressed as a percentage of expression of *Hprt1* and are representative of two separate experiments. *, $P < 0.05$ (two-tailed Student's *t*-test).

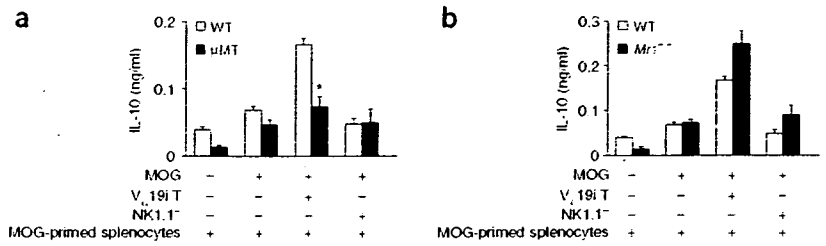

Figure 6 V_α19i T cell–induced IL-10 production is partially B cell dependent but completely MR1 independent. Cytometric bead assay of IL-10 in the supernatants of liver V_α19i T cells from naive V_α19iTg*Cd1d1*$^{-/-}$ mice, cultured for 72 h with MOG(35–55) plus MOG(35–55)-specific splenocytes from wild-type nontransgenic or B cell–deficient μMT mice (**a**) or from wild-type nontransgenic or MR1-deficient mice (**b**). Data represent mean ± s.e.m. of duplicate samples from three independent experiments. *, $P < 0.05$, compared with control (two-tailed Student's *t*-test).

$CD3^+NK1.1^+$ or $CD14^+$ cells using intracellular cytokine flow cytometry. The addition of V_α19i T cells greatly increased IL-10 production by $CD19^+$ B cells and $CD3^+$ $NK1.1^+$ NKT cells (**Fig. 5a**). $CD4^+$ and $CD8^+$ T cells also showed slight increases in IL-10 production in the presence of V_α19i T cells. To demonstrate that B cells were the main IL-10 producing cells *in vivo*, we extracted RNA from sorted splenic $CD4^+$ T cells or $CD19^+$ B cells from V_α19iTg*Cd1d1*$^{-/-}$ or nontransgenic mice with EAE (**Fig. 5b**). In agreement with the results of the *in vitro* coculture system, we found that B cells isolated from V_α19iTg*Cd1d1*$^{-/-}$ mice had higher expression of mRNA transcripts encoding IL-10 than did T cells (**Fig. 5b**). In addition, B cells from V_α19iTg*Cd1d1*$^{-/-}$ mice had higher expression of *Il10* transcripts than did B cells from *Cd1d1*$^{-/-}$ mice (**Fig. 5b**). In contrast, $CD4^+$ T cells from V_α19iTg*Cd1d1*$^{-/-}$ mice had lower expression of T_H1 cytokine–encoding mRNA transcripts than did $CD4^+$ T cells from *Cd1d1*$^{-/-}$ mice (**Fig. 5b**).

To determine if V_α19i T cell–B cell interactions are essential for IL-10 production in the coculture system, we immunized B cell–deficient (μMT) mice with MOG(35–55) to obtain a source of MOG-primed spleen cells lacking B cells. After culture together with V_α19i T cells, B cell–deficient splenocytes produced less IL-10 than did wild-type nontransgenic splenocytes (**Fig. 6a**). As μMT knockout mice may have unusual follicular architecture, to exclude potential indirect effects we repeated these coculture experiments using B cell–depleted wild-type nontransgenic splenocyte samples. B cell–depleted splenocyte samples produced less IL-10 than did nondepleted splenocyte samples whereas the readdition of wild-type B cells to B cell–depleted splenocyte samples restored IL-10 production (56.3 ± 1.2 pg/ml for B cell–depleted splenocyte samples; 126.0 ± 4.4 pg/ml for B cell–depleted splenocyte samples with B cells 'added back'; and 170.4 ± 0.8 pg/ml for nondepleted splenocyte samples).

We hypothesized that an interaction between MR1 on B cells and the V_α19i TCR on T cells could induce IL-10 secretion from both cell types. To test that, we immunized *Mr1*$^{-/-}$ mice with MOG(35–55), followed by coculture experiments. In the absence of MR1, V_α19i T cell–mediated IL-10 production was not reduced (**Fig. 6b**). These results suggest that V_α19i T cell-induced IL-10 production can occur at least in part through MR1-independent interaction with B cells. However, non–B cells also seem to contribute to V_α19i T cell–induced IL-10 production.

Costimulation in V_α19i T cell-induced IL-10 production

Naive V_α19i T cells from V_α19iTg*Cd1d1*$^{-/-}$ mice expressed more of the costimulatory molecules CD278 (ICOS), CD86 (B7-2), CD154 (CD40L) and CD28 than did naive splenic T cells (**Fig. 7a**). V_α19i T cells also expressed CD44 more 'brightly' than did naive T cells (data not shown). These results indicate that V_α19i T cells have an activated or memory phenotype, similar to that of V_α14i NKT cells[1] and 'mucosal-associated invariant T cells' isolated from gut mucosa[2].

Given that MR1 is not required for IL-10 production, we hypothesized that costimulatory interactions may provide the stimulus for IL-10 production. To test that, we repeated the coculture experiments in the presence of blocking antibodies specific for the costimulatory molecules B7RP-1, CD80, CD86 and CD40L. We found that blockade of each costimulatory pathway resulted in significantly lower IL-10 secretion than that of control cocultures treated with control immunoglobulin (**Fig. 7b**). However, blockade of the ICOS–B7RP-1 pathway inhibited IL-10 production most substantially. To extend those

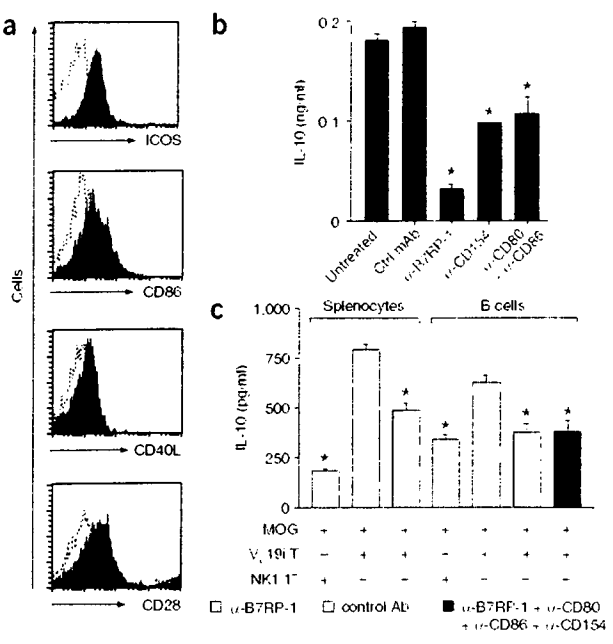

Figure 7 ICOS–B7RP-1 costimulation contributes to V_α19i T cell–induced B cell IL-10 production. (**a**) Flow cytometry of costimulatory molecule expression on the surface of liver V_α19i T cells (filled histograms) and naive splenic T cells from C57BL/6 mice (dotted lines). Data are representative of three separate experiments. (**b**) Cytometric bead assay of IL-10 in the supernatants of liver V_α19i T cells from naive mice, cultured with MOG(35–55) and MOG(35–55)-specific splenocytes from wild-type nontransgenic EAE mice in the presence of isotype-matched control antibody (Ctrl mAb) or of blocking antibodies specific to various costimulatory molecules (α-; below graph), measured after 72 h of incubation. Data are representative of two separate experiments. (**c**) Cytometric bead assay of IL-10 in the supernatants of liver V_α19i T cells from naive V_α19iTg*Cd1d1*$^{-/-}$ mice, cultured with MOG(35–55) and MOG(35–55)-specific splenocytes or sorted B cells from wild-type nontransgenic EAE mice in the presence of various antibodies (key), measured after 72 h of incubation. *, $P < 0.001$, compared with control groups (analysis of variance). Data represent mean ± s.e.m. of triplicate samples from two separate experiments.

findings further, we cultured V_α19i T cells together with purified B cells. This resulted in B7RP-1-dependent IL-10 production (**Fig. 7c**). B7RP-1 blockade partially inhibited IL-10 production in cocultures of V_α19i T cells and splenocytes and fully inhibited IL-10 production in cocultures of V_α19i T cells and purified B cells (**Fig. 7c**). These results suggest that although B cells are a chief producer of IL-10 in this system, other cell types also contribute to V_α19i T cell–induced IL-10 production. Furthermore, the ICOS–B7RP-1 pathway is vital for V_α19i T cell–induced, B cell–mediated IL-10 production, as blockade with a combination of antibodies to costimulatory molecules (B7RP-1, CD80, CD86 and CD40L) inhibited IL-10 to the same degree as anti-B7RP-1 alone (**Fig. 7c**). However, other costimulatory molecules are involved in V_α19i T cell–induced IL-10 production from whole splenocytes (**Fig. 7b**).

DISCUSSION

Although T cells expressing the invariant V_α19-J_α33 TCR chain were first identified in 1993 (ref. 22), knowledge of the immunological function of this invariant T cell population is still limited. Nevertheless, important characteristics of this lymphocyte subset have been characterized, including their restriction by MR1, their TAP (transporter associated with antigen processing)–independent development in rodents, humans and cattle, and the notable interspecies conservation of this invariant TCR. Because CD1d-restricted V_α14i NKT cells, which influence autoimmunity, have similar properties, we speculated that MR1-resricted T cells would also be capable of modifying autoimmunity. However, V_α19i T cells are distinct from V_α14i CD1d-restricted T cells in their 'preferential' distribution in the gut mucosa and their dependence on the presence of B cells and gut flora.

V_α7.2i T cells, the human homolog of V_α19i T cells, are present in lesions of patients with multiple sclerosis[25]. As multiple sclerosis is a demyelinating disease involving autoimmune T cells, B cells, macrophages and various inflammatory mediators, it is possible that MR1-restricted T cells may regulate ongoing disease activity in the CNS. Using an animal model of multiple sclerosis, we examined the effect of overexpression or deletion of MR1-restricted T cells on disease course and severity. Our study suggests that V_α19i T cells can suppress autoimmune inflammation. In addition, we have shown that V_α19i T cells have a memory or activated surface phenotype and are able to produce large amounts of T_H1 and T_H2 cytokines. NK1.1$^+$ T cells from V_α19iTg mice produced more cytokines than did NK1.1$^+$ T cells from V_α19iTg*Cd1d1*$^{-/-}$ mice, indicating a possible interaction between CD1d- and MR1-restricted lymphocytes.

We undertook several approaches to determine whether V_α19i T cells regulate EAE pathogenesis. Overexpression of V_α19i T cells protected mice from clinical EAE. Inhibition of EAE was associated with reduced infiltration and demyelination of the spinal cord as well as a decrease in the production of disease-promoting T_H1 cytokines in the draining lymph nodes and spleen and a reciprocal increase in IL-10, a well established inhibitor of EAE[27–30]. IL-17-secreting cells, which function independently of T_H1 cells, may promote EAE[31]. Here we determined that the inhibitory effect of V_α19i T cells is biased toward prevention of secretion of T_H1 cytokines rather than IL-17.

A potential limitation of TCR-transgenic models is the possible disruption of conventional TCR diversity, which could skew TCR recognition of MOG. However, this is unlikely, as anti-MOG T cell proliferative responses were similar in wild-type nontransgenic and V_α19iTg mice. Furthermore, we adoptively transferred liver V_α19i T cells from naive V_α19iTg*Cd1d1*$^{-/-}$ mice into wild-type nontransgenic mice with EAE, which express natural TCR diversity. In those experiments, V_α19i T cells effectively inhibited EAE, suggesting that V_α19i T cells have a regulatory function during EAE. However, a potential limitation of our model is the difficulty of obtaining pure V_α19i T cell preparations because of the lack of a V_α19 TCR–specific antibody. Therefore, experiments using sorted CD3$^+$ NK1.1$^+$ cells from V_α19iTg*Cd1d1*$^{-/-}$ mice may also contain small numbers of non-V_α14i TCR NK1.1$^+$ T cells of other TCR specificities. To ascertain whether normal numbers of V_α19i T cells in wild-type nontransgenic mice could be involved during EAE, we induced EAE in *Mr1*$^{-/-}$ mice and found that the absence of V_α19i T cells resulted in a more severe clinical disease than that of wild-type nontransgenic mice.

V_α19i T cells most likely exert their main effects in the peripheral lymphoid tissue, as the reduction in proinflammatory cytokines and increase in IL-10 was in the draining lymph nodes and spleen. We also demonstrated that the protective effect of V_α19i T cells was independent of V_α14i NKT cells by using V_α19iTg mice on a CD1d-deficient background. Notably, we found reduced adhesion molecule expression on effector T cells from V_α19iTg*Cd1d1*$^{-/-}$ mice, which correlated with reduced T cell infiltration of the CNS. However, we did note low numbers of V_α19i T cells (CD3$^+$NK1.1$^+$ from V_α19iTg*Cd1d1*$^{-/-}$mice) and B cells in the CNS of mice with EAE, suggesting that V_α19i T cells may also regulate EAE in the CNS.

Coculture experiments suggested that IL-10-producing B cells are involved in the amelioration of EAE in V_α19iTg*Cd1d1*$^{-/-}$ mice. Notably, that finding is consistent with published studies demonstrating that IL-10-producing B cells are involved in spontaneous remission from EAE and could limit clinical disease when adoptively transferred into mice with EAE[32] or a model of collagen-induced arthritis[33]. However, those results do not exclude the possibility that *in vivo*, other cell types are also involved in V_α19i T cell–mediated immune regulation. B cells express MR1 (ref. 34), and V_α19i T cells are MR1 restricted[7], but IL-10 production was unaffected in coculture experiments with lymphocytes from MR1-deficient mice, suggesting that MR1, although necessary for V_α19i T cell selection, is not essential for V_α19i T cell–induced B cell IL-10 production.

T cell activation requires TCR stimulation as well as costimulatory signals. Many costimulatory molecules that regulate cell activation and cytokine secretion have been identified: ICOS and its ligand B7RP-1, CD40-CD40L and CD28-CD80 and CD28-CD86 (refs. 35–38). ICOS costimulation induces IL-10 production as well as help for B cell maturation and CD40L expression[39,40]. The expression of costimulatory molecules on V_α19i T cells was unknown before; we have demonstrated here that V_α19i T cells express ICOS, CD28, CD86 and CD40L. To determine the contribution of each of these costimulatory signaling pathways on the production of IL-10 after V_α19i T cell–B cell interactions, we repeated the coculture experiments using blocking monoclonal antibody to each of the costimulatory pathways. We found that blockade of the ICOS–B7RP-1 pathway inhibited IL-10 production. Furthermore, blockade of the CD40-CD40L, CD28-CD80 or CD28-CD86 pathway also blocked IL-10 production, although not to the extent seen with ICOS blockade.

Commensal flora in the gut are important for the selection of V_α19i T cells[7]. V_α19i T cells may also control gut production of immunoglobulin A from B cells, suggesting involvement of V_α19i T cells in intestinal B cell regulation[7]. Additionally, IL-10 is important for inhibiting excessive inflammation toward gut flora[41], and it has been shown that IL-10 and transforming growth factor-β are involved in immunoglobulin A synthesis and secretion[42]. In the presence of IL-10 and CD40-CD40L signaling, production of immunoglobulin A is increased[43]. Thus, our findings presented here are consistent with the hypothesis that V_α19i T cells are involved in the homeostasis of gut immunity[2,7]. We have shown that V_α19i T cells help B cells produce

IL-10, which in nonpathogenic conditions may inhibit inflammation against gut flora required for V_α19i T cell selection. Therefore, we propose a model of V_α19i T cell–induced protection from EAE whereby V_α19i T cells interact with B cells in lymphoid tissue through ICOS–B7RP-1 and to a lesser degree through other costimulatory pathways to induce IL-10 production, which in turn can inhibit the production of disease-promoting T_H1 cytokines such as IFN-γ and TNF. In conclusion, here we have identified a protective function for invariant V_α19i T cells in autoimmune disease. In contrast to 'conventional' V_α14i NKT cells, more T cells express the V_α19i TCR human homolog V_α7.2-J_α33 than in mice and therefore these cells may prove to be useful therapeutic targets for the treatment of autoimmune disease.

METHODS

Mice and induction of EAE. C57BL/6 mice (CLEA Laboratory Animal), μMT mice (Jackson Laboratories), V_α19iTg mice[5], V_α19iTg*Cd1d1*$^{-/-}$ mice, *Cd1d1*$^{-/-}$ mice and *Mr1*$^{-/-}$ mice[7] were maintained in specific pathogen–free conditions in accordance with institutional guidelines (National Institute of Neuroscience, Tokyo, Japan.). *Mr1*$^{-/-}$ mice were backcrossed to C57BL/6 mice for ten generations[24]. Mice were injected subcutaneously with 100 μg MOG(35–55) and 1 mg heat-killed *Mycobacterium tuberculosis* H37RA (Difco) emulsified in complete Freund's adjuvant. Pertussis toxin (200 ng in PBS; List .Biological Laboratories) was injected intraperitoneally on days 0 and 2 after immunization. EAE clinical symptoms were assigned scores daily as follows: 0, no clinical signs; 1, loss of tail tonicity; 2, impaired righting reflex; 3, partial hindlimb paralysis; 4, total hindlimb paralysis.

Cell sorting and adoptive transfer. For depletion of NK cells, mice were injected intraperitoneally with 100 μg anti-asialo-GM_1 (ref. 44) 48 h before purification of V_α19i T cells. Liver or spleen cells were isolated from mice by Percoll density-gradient centrifugation, and NKT cells, B cells and T cells were purified with the AutoMACS cell purification system (Miltenyi Biotech). NKT cells were isolated using phycoerythrin-conjugated anti-NK1.1 (PK136; BD Pharmingen) and anti-phycoerythrin microbeads (Miltenyi Biotech). The purity of isolated NK1.1$^+$ T cells, assessed by flow cytometry, was more than 90%. In some experiments, single-cell suspensions were incubated with fluorescein isothiocyanate–anti-CD3 (2C11; BD Pharmingen) and phycoerythrin–anti-NK1.1 (PK136, BD Pharmingen) for sorting by flow cytometry. B cells and T cells were isolated from the spleen with anti-CD19 microbeads or the 'pan T cell' kit (Miltenyi Biotech). For adoptive transfer studies, liver CD3$^+$NK1.1$^+$ V_α19i T cells were sorted from naive V_α19iTg*Cd1d1*$^{-/-}$ mice as described above, and 1×10^6 V_α19i T cells were injected intraperitoneally into naive C57BL/6 recipient mice on the day of immunization with MOG(35–55). Control groups received identical numbers of CD3$^+$NK1.1$^-$ hepatic cells.

Cell proliferation and cytokine analysis. For *in vitro* stimulation of sorted V_α19i T cells, CD3$^+$NK1.1$^+$ and CD3$^+$NK1.1$^-$ cells were suspended in RPMI 1640 medium (Sigma) supplemented with 10% FCS, 2 mM L-glutamine, 100 U/ml of penicillin-streptomycin, 2 mM sodium pyruvate and 50 μM β-mercaptoethanol and were stimulated with immobilized anti-CD3 (5 μg/ml; BD Pharmingen). Cytokines were measured with inflammation cytometric bead assay kits (BD Biosciences) at 24, 48 and 72 h after stimulation with mouse T_H1-T_H2 cytokines. At 10 d after EAE induction without pertussis toxin, myelin-specific T cell responses were measured. Lymphocytes (1×10^6) were cultured with MOG(35–55) (1–100 μM for proliferation studies and 100 μM for cytokine analysis). Cytokines were measured with a cytometric bead assay kit (BD Biosciences) or an IL-17 enzyme-linked immunosorbent assay kit (BD Pharmingen) at 72 h after stimulation. Identical sets of wells were used for proliferation studies. After 72 h, cells were incubated with [^{3}H]thymidine (1 μCi/well) for the final 16 h of culture and incorporation of radioactivity was analyzed with a β-1205 counter (Pharmacia). Proliferation was determined from triplicate wells for each peptide concentration and is expressed as counts per minute.

Surface marker analysis, quantification of CNS leukocytes and histology. The surface phenotype of sorted V_α19i T cells was analyzed by flow cytometry. Nonspecific staining was inhibited by incubation with anti-CD16/32 (BD Pharmingen). Cells were then stained with fluorescence-labeled antibodies specific for CD4, NK1.1, TCRβ, CD3, CD44, CD49d, CD19, CD8, CD14, CD28, CD278, CD86 or CD154 (BD Pharmingen) or CCR1 and CCR2 (Santa Cruz), followed by phycoerythrin-conjugated anti–goat immunoglobulin G (Santa Cruz), and were analyzed with a FACSCalibur (Becton Dickinson). Intracellular cytokines were analyzed by flow cytometry with the BD Cytofix/Cytoperm kit (BD Pharmingen). Staining of paraffin-embedded spinal cords with luxol fast blue and with haematoxylin and eosin was done by SRL. For quantification by flow cytometry, spinal cords were homogenized through 70-μm nylon mesh and by Percoll density-gradient centrifugation to form single-cell suspensions.

RNA extraction and real-time RT-PCR. The SV Total RNA isolation kit (Promega) was used for isolation of total RNA from sorted liver or splenic NKT cells, T cells or B cells according to the manufacturer's instructions. First-strand cDNA was generated with the Advantage-RT kit (Clontech). The Light Cycler-FastStart DNA Master SYBR Green I kit (Roche Diagnostics) was used for real-time PCR. Gene expression values were normalized to expression of the hypoxanthine guanine phosphoribosyl transferase (*Hprt1*) 'housekeeping' gene. Primers from Bex Co are listed in **Supplementary Table 1** online.

Mixed-lymphocyte experiments. MOG(35–55)-specific spleen cells (2×10^6) isolated from wild-type nontransgenic mice 10 d after EAE induction were mixed with liver V_α19i T cells (5×10^5) sorted from naive V_α19iTg*Cd1d1*$^{-/-}$ mice, in the presence of 100 μg/ml of MOG(35–55) in 24-well plates or transwell plates (Corning). Where indicated, MOG(35–55)-specific spleen cells were isolated from *Mr1*$^{-/-}$ or μMT mice or were subjected to depletion with anti-CD19 microbeads (Miltenyi Biotech). Costimulatory molecules were blocked with 10 μg/ml of anti-B7RP-1 (HK5.3) or anti-CD40L (MR1) or with anti-CD80 and anti-CD86 (16-10A1 and GL1, respectively; all from BD Pharmingen)[35]. After 72 h, cytokines in the supernatant were analyzed by cytometric bead assay, enzyme-linked immunosorbent assay or intracellular flow cytometry. Proliferation of MOG(35–55)-specific lymph node cells was assessed 24 h after the addition of [^{3}H]thymidine (1 μCi/well) to 96-well plates.

Statistics. EAE clinical scores for groups of mice are presented as the mean group clinical score ± s.e.m., and statistical differences were analyzed by the Mann-Whitney U nonparametric ranking test. Cytokine secretion data were analyzed with the two-tailed Student's *t*-test or one-way analysis of variance with Tukey post-analysis for multiple group analysis.

Note: Supplementary information is available on the Nature Immunology website.

ACKNOWLEDGMENTS

We thank S. Gilfillan (Department of Pathology and Immunology, Washington University School of Medicine, St. Louis, Missouri) for *Mr1*$^{-/-}$ mice. Supported by the Japan Society for the Promotion of Science (P03581 to J.L.C), the Ministry of Health, Labour and Welfare of Japan (T.Y. and S.M.), The Program for Promotion of Fundamental Studies in Health Sciences of the National Institute of Biomedical Innovation (02-5 to T.Y.), Grant-in-Aid for Science Research on Priority Area from Ministry of Education, Science, Sports and Culture of Japan (17047051 to S.M.) and Grant-in-Aid for Scientific Research (B) (18390295 to S.M.) from the Japan Society for the Promotion of Science.

COMPETING INTERESTS STATEMENT

The authors declare that they have no competing financial interests.

Published online at http://www.nature.com/natureimmunology/
Reprints and permissions information is available online at http://npg.nature.com/reprintsandpermissions/

1. Kronenberg, M. Toward an understanding of NKT cell biology: progress and paradox. *Annu. Rev. Immunol.* **23**, 877–900 (2005).
2. Treiner, E. *et al.* Mucosal-associated invariant T (MAIT) cells: an evolutionarily conserved T cell subset. *Microbes Infect.* **7**, 552–559 (2005).
3. Kawano, T. *et al.* CD1d-restricted and TCR-mediated activation of Vα14 NKT cells by glycosylceramides. *Science* **278**, 1626–1629 (1997).

4. Zhou, D. *et al.* Lysosomal glycosphingolipid recognition by NKT cells. *Science* **306**, 1786–1789 (2004).
5. Okamoto, N. *et al.* Synthetic α-mannosyl ceramide as a potent stimulant for an NKT cell repertoire bearing the invariant $V_{\alpha}19$-$J_{\alpha}26$ TCR α chain. *Chem. Biol.* **12**, 677–683 (2005).
6. Chen, Y.H., Chiu, N.M., Mandal, M., Wang, N. & Wang, C.R. Impaired $NK1^+$ T cell development and early IL-4 production in CD1-deficient mice. *Immunity* **6**, 459–467 (1997).
7. Treiner, E. *et al.* Selection of evolutionarily conserved mucosal-associated invariant T cells by MR1. *Nature* **422**, 164–169 (2003).
8. Spada, F.M., Koezuka, Y. & Porcelli, S.A. CD1d-restricted recognition of synthetic glycolipid antigens by human natural killer T cells. *J. Exp. Med.* **188**, 1529–1534 (1998).
9. Tilloy, F. *et al.* An invariant T cell receptor α chain defines a novel TAP-independent major histocompatibility complex class Ib-restricted α/β T cell subpopulation in mammals. *J. Exp. Med.* **189**, 1907–1921 (1999).
10. Godfrey, D.I., MacDonald, H.R., Kronenberg, M., Smyth, M.J. & Van Kaer, L. NKT cells: what's in a name? *Nat. Rev. Immunol.* **4**, 231–237 (2004).
11. Lehuen, A. *et al.* Overexpression of natural killer T cells protects Vα14-Jα281 transgenic nonobese diabetic mice against diabetes. *J. Exp. Med.* **188**, 1831–1839 (1998).
12. Mars, L.T. *et al.* Vα14-Jα281 NKT cells naturally regulate experimental autoimmune encephalomyelitis in nonobese diabetic mice. *J. Immunol.* **168**, 6007–6011 (2002).
13. Wagner, M.J., Hussain, S., Mehan, M., Verdi, J.M. & Delovitch, T.L. A defect in lineage fate decision during fetal thymic invariant NKT cell development may regulate susceptibility to type 1 diabetes. *J. Immunol.* **174**, 6764–6771 (2005).
14. Pál, E. *et al.* Costimulation-dependent modulation of experimental autoimmune encephalomyelitis by ligand stimulation of Vα14 NK T cells. *J. Immunol.* **166**, 662–668 (2001).
15. Sharif, S. *et al.* Activation of natural killer T cells by α-galactosylceramide treatment prevents the onset and recurrence of autoimmune type 1 diabetes. *Nat. Med.* **7**, 1057–1062 (2001).
16. Hong, S. *et al.* The natural killer T-cell ligand α-galactosylceramide prevents autoimmune diabetes in non-obese diabetic mice. *Nat. Med.* **7**, 1052–1056 (2001).
17. Miyamoto, K., Miyake, S. & Yamamura, T. A synthetic glycolipid prevents autoimmune encephalomyelitis by inducing T_H2 bias of natural killer T cells. *Nature* **413**, 531–534 (2001).
18. Chiba, A. *et al.* Suppression of collagen-induced arthritis by natural killer T cell activation with OCH, a sphingosine-truncated analog of α-galactosylceramide. *Arthritis Rheum.* **50**, 305–313 (2004).
19. Miyake, S. & Yamamura, T. Therapeutic potential of glycolipid ligands for natural killer (NK) T cells in the suppression of autoimmune diseases. *Curr. Drug Targets Immune Endocr. Metabol. Disord.* **5**, 315–322 (2005).
20. Chiba, A., Kaieda, S., Oki, S., Yamamura, T. & Miyake, S. The involvement of Vα14 natural killer T cells in the pathogenesis of arthritis in murine models. *Arthritis Rheum.* **52**, 1941–1948 (2005).
21. Kim, H.Y. *et al.* NKT cells promote antibody-induced joint inflammation by suppressing transforming growth factor β1 production. *J. Exp. Med.* **201**, 41–47 (2005).
22. Porcelli, S., Yockey, C.E., Brenner, M.B. & Balk, S.P. Analysis of T cell antigen receptor (TCR) expression by human peripheral blood $CD4^-8^-$ α/β T cells demonstrates preferential use of several V_{β} genes and an invariant TCR α chain. *J. Exp. Med.* **178**, 1–16 (1993).
23. Shimamura, M. & Huang, Y.Y. Presence of a novel subset of NKT cells bearing an invariant Vα19.1-Jα26 TCR α chain. *FEBS Lett.* **516**, 97–100 (2002).
24. Kawachi, I., Maldonado, J., Strader, C. & Gilfillan, S. MR1-restricted Vα19i mucosal-associated invariant T cells are innate T cells in the gut lamina propria that provide a rapid and diverse cytokine response. *J. Immunol.* **176**, 1618–1627 (2006).
25. Illés, Z., Shimamura, M., Newcombe, J., Oka, N. & Yamamura, T. Accumulation of Vα7.2-Jα33 invariant T cells in human autoimmune inflammatory lesions in the nervous system. *Int. Immunol.* **16**, 223–230 (2004).
26. Illés, Z. *et al.* Differential expression of NK T cell Vα24JαQ invariant TCR chain in the lesions of multiple sclerosis and chronic inflammatory demyelinating polyneuropathy. *J. Immunol.* **164**, 4375–4381 (2000).
27. Croxford, J.L., Feldmann, M., Chernajovsky, Y. & Baker, D. Different therapeutic outcomes in experimental allergic encephalomyelitis dependent upon the mode of delivery of IL-10: a comparison of the effects of protein, adenoviral or retroviral IL-10 delivery into the central nervous system. *J. Immunol.* **166**, 4124–4130 (2001).
28. Croxford, J.L. *et al.* Cytokine gene therapy in experimental allergic encephalomyelitis by injection of plasmid DNA-cationic liposome complex into the central nervous system. *J. Immunol.* **160**, 5181–5187 (1998).
29. Cua, D.J., Groux, H., Hinton, D.R., Stohlman, S.A. & Coffman, R.L. Transgenic interleukin 10 prevents induction of experimental autoimmune encephalomyelitis. *J. Exp. Med.* **189**, 1005–1010 (1999).
30. Bettelli, E., Nicholson, L.B. & Kuchroo, V.K. IL-10, a key effector regulatory cytokine in experimental autoimmune encephalomyelitis. *J. Autoimmun.* **20**, 265–267 (2003).
31. Langrish, C.L. *et al.* IL-23 drives a pathogenic T cell population that induces autoimmune inflammation. *J. Exp. Med.* **201**, 233–240 (2005).
32. Fillatreau, S., Sweenie, C.H., McGeachy, M.J., Gray, D. & Anderton, S.M. B cells regulate autoimmunity by provision of IL-10. *Nat. Immunol.* **3**, 944–950 (2002).
33. Mauri, C., Gray, D., Mushtaq, N. & Londei, M. Prevention of arthritis by interleukin 10-producing B cells. *J. Exp. Med.* **197**, 489–501 (2003).
34. Riegert, P., Wanner, V. & Bahram, S. Genomics, isoforms, expression, and phylogeny of the MHC class I-related MR1 gene. *J. Immunol.* **161**, 4066–4077 (1998).
35. Hayakawa, Y. *et al.* Differential regulation of Th1 and Th2 functions of NKT cells by CD28 and CD40 costimulatory pathways. *J. Immunol.* **166**, 6012–6018 (2001).
36. Ikarashi, Y. *et al.* Dendritic cell maturation overrules H-2D-mediated natural killer T (NKT) cell inhibition: critical role for B7 in CD1d-dependent NKT cell interferon γ production. *J. Exp. Med.* **194**, 1179–1186 (2001).
37. Kitamura, H. *et al.* The natural killer T (NKT) cell ligand α-galactosylceramide demonstrates its immunopotentiating effect by inducing interleukin (IL)-12 production by dendritic cells and IL-12 receptor expression on NKT cells. *J. Exp. Med.* **189**, 1121–1128 (1999).
38. Kaneda, H. *et al.* ICOS costimulates invariant NKT cell activation. *Biochem. Biophys. Res. Commun.* **327**, 201–207 (2005).
39. Hutloff, A. *et al.* ICOS is an inducible T-cell co-stimulator structurally and functionally related to CD28. *Nature* **397**, 263–266 (1999).
40. McAdam, A.J. *et al.* ICOS is critical for CD40-mediated antibody class switching. *Nature* **409**, 102–105 (2001).
41. Song, F. *et al.* Expression of the neutrophil chemokine KC in the colon of mice with enterocolitis and by intestinal epithelial cell lines: effects of flora and proinflammatory cytokines. *J. Immunol.* **162**, 2275–2280 (1999).
42. Kaneko, M., Akiyama, Y., Takimoto, H. & Kumazawa, Y. Mechanism of up-regulation of immunoglobulin A production in the intestine of mice unresponsive to lipopolysaccharide. *Immunology* **116**, 64–70 (2005).
43. Cognasse, F. *et al.* Differential downstream effects of CD40 ligation mediated by membrane or soluble CD40L and agonistic Ab: a study on purified human B cells. *Int. J. Immunopathol. Pharmacol.* **18**, 65–74 (2005).
44. Muhlen, K.A. *et al.* NK cells, but not NKT cells, are involved in *Pseudomonas aeruginosa* exotoxin A-induced hepatotoxicity in mice. *J. Immunol.* **172**, 3034–3041 (2004).

Differential Expression of CD11c by Peripheral Blood NK Cells Reflects Temporal Activity of Multiple Sclerosis[1]

Toshimasa Aranami, Sachiko Miyake, and Takashi Yamamura[2]

Multiple sclerosis (MS) is an autoimmune disease, showing a great degree of variance in temporal disease activity. We have recently demonstrated that peripheral blood NK cells biased for secreting IL-5 (NK2 bias) are associated with the remission state of MS. In this study, we report that MS patients in remission differentially express CD11c on NK cell surface (operationally defined as $CD11c^{high}$ or $CD11c^{low}$). When we compared $CD11c^{high}$ or $CD11c^{low}$ patients, the expression of IL-5 and GATA-3 in NK cells supposed to endow a disease-protective NK2 phenotype was observed in $CD11c^{low}$ but not in $CD11c^{high}$ patients. In contrast, the $CD11c^{high}$ group showed a higher expression of HLA-DR on NK cells. In vitro studies demonstrated that NK cell stimulatory cytokines such as IL-15 would up-regulate CD11c expression on NK cells. Given previous evidence showing an association between an increased level of proinflammatory cytokines and temporal disease activity in MS, we postulate that inflammatory signals may play a role in inducing the $CD11c^{high}$ NK cell phenotype. Follow-up of a new cohort of patients showed that 6 of 10 $CD11c^{high}$ MS patients developed a clinical relapse within 120 days after evaluation, whereas only 2 of 13 $CD11c^{low}$ developed exacerbated disease ($p = 0.003$). As such, a higher expression of CD11c on NK cells may reflect the temporal activity of MS as well as a loss of regulatory NK2 phenotype, which may allow us to use it as a potential biomarker to monitor the immunological status of MS patients. ***The Journal of Immunology*****, 2006, 177: 5659–5667.**

Multiple sclerosis (MS)[3] is a chronic inflammatory disease of the CNS, in which autoreactive T cells targeting CNS Ags are presumed to play a pathogenic role (1). A large majority of the patients with MS (~70%), known as relapsing-remitting MS, would develop acute exacerbations of disease between intervals of remission. It is currently believed that relapses are caused by T cell- and Ab-mediated inflammatory reactions to the self-CNS components, and could be controlled at least to some degree by anti-inflammatory therapeutics, immunosuppressants, or plasma exchange.

The clinical course of MS varies greatly among individuals, implicating difficulties to predict the future of each patient. For example, patients who had been clinically inactive in the early stage of illness could abruptly change into active MS accompanying frequent relapses and progressive worsening of neurological conditions. There are a number of unpredictable matters in MS, including an interval between relapses, responsiveness to remedy and the prognosis in terms of neurological disability. To provide better quality of management of the patients, searches of appropriate biomarkers are currently being warranted (2).

We have recently shown that surface phenotype and cytokine secretion pattern of peripheral blood NK cells may reflect the disease activity of MS (3, 4). A combination of quantitative PCR and flow cytometry analysis has revealed that NK cells in clinical remission of MS are characterized by a higher frequency of $CD95^+$ cells as well as a higher expression level of IL-5 than those of healthy subjects (HS) (3). As IL-5-producing NK cells, referred to as NK2 cells (5), could prohibit Th1 cell activation in vitro (3), we interpreted that the NK2 bias in MS may contribute to maintaining the remission state of MS. More recently, we have found that MS patients in remission can be further divided into $CD95^{high}$ and $CD95^{low}$, according to the frequency of $CD95^+$ cells among NK cells (4). Notably, memory T cells reactive to myelin basic protein, a major target Ag in MS, were increased in $CD95^{high}$ patients, compared with $CD95^{low}$. Of note, $CD95^{high}$ NK cells exhibited an ability to actively suppress the autoimmune T cells, whereas those from $CD95^{low}$ patients did not. These results suggest that NK cells may accommodate their function and phenotype to properly counterregulate autoimmune T cells in the remission state of MS.

Recently, a distinct population of NK cells that express CD11c, a prototypical dendritic cell (DC) marker, was identified in mice (6, 7). As the $CD11c^+$ NK cells exhibited both NK and DC functions, they are called as "bitypic NK/DC cells." CD11c associates with integrin CD18 to form CD11c/CD18 complex and is expressed on monocytes, granulocytes, DCs, and a subset of NK cells. Although precise functions are unclear, it has been reported that CD11c is involved in binding of iC3b (8), adhesion to stimulated endothelium (9) or phagocytosis of apoptotic cells (10). The initial purpose of this study was to evaluate CD11c expression and function of $CD11c^+$ NK cells in MS in the line of our research to characterize NK cells in MS. On initiating study, we noticed that there was no significant difference between MS and HS in the frequency of $CD11c^+$ NK cells. However, expression levels of CD11c were significantly higher in MS. We further noticed that up-regulation of CD11c is seen in some, but not all, patients with MS. So we have operationally classified MS into $CD11c^{low}$ and $CD11c^{high}$.

In this study, we demonstrate that IL-5, characteristic of NK2 cells (5), were significantly down-regulated in $CD11c^{high}$ than

Department of Immunology, National Institute of Neuroscience, National Center of Neurology and Psychiatry, Tokyo, Japan

Received for publication May 3, 2006. Accepted for publication July 28, 2006.

The costs of publication of this article were defrayed in part by the payment of page charges. This article must therefore be hereby marked *advertisement* in accordance with 18 U.S.C. Section 1734 solely to indicate this fact.

[1] This work was supported by grants from the Ministry of Health, Labor and Welfare of Japan and the Program for Promotion of Fundamental Studies in Health Sciences of the National Institute of Biomedical Innovation.

[2] Address correspondence and reprint requests to Dr. Takashi Yamamura, Department of Immunology, National Institute of Neuroscience, National Center of Neurology and Psychiatry, 4-1-1 Ogawahigashi, Kodaira, Tokyo 187-8502, Japan. E-mail address: yamamura@ncnp.go.jp

[3] Abbreviations used in this paper: MS, multiple sclerosis; HS, healthy subject; DC, dendritic cell; MFI, mean fluorescence intensity; ECD, energy-coupled dye.

0022-1767/06/$02.00

$CD11c^{low}$ NK cells. In contrast, expression of HLA-DR class II molecule was up-regulated in $CD11c^{high}$ NK cells. Notably, both CD11c and HLA-DR on NK cells were reproducibly induced in vitro in the presence of IL-15 (11) or combination of inflammatory cytokines, known to be increased in the blood of MS (12–14). Furthermore, we found that the remission state of $CD11c^{high}$ is unstable in comparison to $CD11c^{low}$, as judged by an increased number of the patients who exacerbated during the 120 days after examining NK cell phenotypes. These results suggest that the $CD11c^{high}$ group of patients may be in more unstable condition than $CD11c^{low}$, presenting with reduced regulatory functions of NK cells.

Materials and Methods

Subjects

Twenty-five patients with relapsing-remitting MS (15) (male (M)/female (F) = 8/17; age = 37.7 ± 11.1 (year old)) and 10 sex- and age-matched HS (M/F = 3/7; age = 39.9 ± 12.2 (year old)) were enrolled for studying NK cell phenotypes. All the patients were in the state of remission at examination as judged by magnetic resonance imaging scanning and clinical assessment. They had not been given immunosuppressive medications, or corticosteroid for at least 1 mo before examination. They had relatively mild neurological disability (expanded disability status scale <4) and could walk to the hospital without any assistance during remission. The same neurologist followed up the patients regularly (every 3–4 wk) and judged the occurrence of relapse by using magnetic resonance imaging and clinical examinations. Information on NK cell phenotype or other immunological parameters was never given to either the neurologist or the patients at the time of evaluation. To precisely determine the onset of relapse, patients were allowed to take examination within a few days after a new symptom appeared. Written informed consent was obtained from all the patients and the Ethics Committee of the National Center of Neuroscience (NCNP) approved the study.

Reagents

Mouse IgG1 isotype control-PE, anti-CD3-energy-coupled dye (ECD), anti-CD4-PE, anti-CD8-PC5, anti-CD56-PC5, anti-CD69-PE, and anti-HLA-DR-FITC mAbs were purchased from Immunotech. Anti-CD11c-PE and anti-CD95-FITC were purchased from BD Pharmingen. Recombinant human cytokines were purchased from PeproTech. AIM-V (Invitrogen Life Technologies) was used for cell culture after supplementing 2 mM L-glutamine, 100 U/ml penicillin, and 100 mg/ml streptomycin (Invitrogen Life Technologies).

Cell preparation and NK cell purification

PBMC were separated by density gradient centrifugation with Ficoll-Hypaque PLUS (Amersham Biosciences). To purify NK cells, PBMC were treated with NK isolation kit II (Miltenyi Biotec) twice, according to the manufacturer's protocol. Briefly, PBMC were labeled with a mixture of biotin-conjugated mAbs reactive to non-NK cells and magnetic microbead-conjugated anti-biotin mAbs. The magnetically labeled non-NK cells were depleted with auto-MACS (Miltenyi Biotec) and this procedure always yielded >95% purity of NK cells when assessed by the proportions of $CD3^-CD56^+$ cells with flow cytometry.

Flow cytometry

To evaluate the expression of CD11c, CD95, or other surface molecules on NK cells, PBMC were stained with anti-CD3-ECD, anti-CD56-PC5, and FITC- or PE-conjugated mAbs against molecules of our interest and were analyzed with EPICS flow cytometry (Beckman Coulter). Mean fluorescence intensity (MFI) of CD11c was measured on gated $CD11c^+$ fraction or whole NK cells.

Stimulation of purified NK cells with proinflammatory cytokines

Purified NK cells (1×10^5/well) were stimulated in the presence or absence of IL-4, IL-8, IL-12, IL-15, IL-18, IL-23, TNF-α, and GM-CSF or combination of IL-12, IL-15, and IL-18 for 3 days. We analyzed CD11c expression after staining the cells with anti-CD11c-PE, anti-CD3-ECD, and anti-CD56-PC5. The concentration of IL-12 was at 10 ng/ml, and those of the other cytokines were at 100 ng/ml.

RT-PCR

Total RNA were extracted with a RNeasy Mini kit (Qiagen) from purified NK cells, and the cDNA were synthesized with Super Script III first strand systems (Invitrogen Life Technologies) according to the manufacturer's protocol. For quantitative analysis of IL-5, IFN-γ, GATA-3, and T-bet, the LightCycler quantitative PCR system (Roche Diagnostics) was used. Relative quantities of mRNA were evaluated after normalizing each expression levels with β-actin expression. PCR primers used were as follows: β-actin-sense, AGAGATGGCCACGGCTGCTT, and -antisense, ATTT GCGGTGGACGATGGAG; IFN-γ-sense, CAGGTCATTCAGATGTA GCG, and -antisense, GCTTTTCGAAGTCATCTCG; IL-5-sense, GCA CACTGGAGAGTCAAACT, and -antisense, CACTCGGTGTTCATTA CACC; GATA-3-sense, CTACGGAAACTCGGTCAGG, and -antisense, CTGGTACTTGAGGCACTCTT; T-bet-sense, GGAGGACACCGACTA ATTTGGGA, and -antisense, AAGCAAGACGCAGCACCAGGTAA.

Statistical analysis of remission rate

We set the first episode of relapse after blood sampling as an end point, although we followed clinical course of each patient for up to 120 days, regardless of whether they developed relapses. No patients developed second relapse during the 120 days. When the neurologist prescribed corticosteroids without knowing any information on the NK cell phenotype, the patient was considered as the dropout at that time point. Remission rate was calculated as Kaplan-Meier survival rate, and statistical difference between $CD11c^{low}$ and $CD11c^{high}$ MS was evaluated with the log-rank test.

Results

CD11c on NK cells is up-regulated in MS remission

First, we confirmed that PBMC from healthy individuals and MS contain $CD11c^+$ NK cells (Fig. 1), which constitute a major population of whole NK cells. We then noticed that proportion of $CD11c^+$ NK cells as well as its levels of expression greatly varied among individuals, particularly in MS. To examine this issue further, we systemically examined 25 MS patients in remission and 10 HS for NK cell expression of CD11c. Whereas 20–80% of NK cells are $CD11c^+$ in HS (Fig. 1*c*), almost all NK cells were $CD11c^+$ in some MS patients (Fig. 1, *c* and *e*). However, reflecting a great degree of variance, comparison between HS and MS did not reveal a significant difference (Fig. 1*c*). In contrast, when we measured the MFI of CD11c expression on $CD11c^+$ NK cells, it was significantly higher in MS as compared with HS (Fig. 1*a*). This difference was also noticed when MFI of CD11c was measured for all the NK cell populations (Fig. 1*b*). It was interesting to know whether the levels of CD11c expression may correlate with NK cell functions. Therefore, we operationally divided the MS patients into $CD11c^{low}$ and $CD11c^{high}$ subgroups (Fig. 1*a*), by setting the border as (the average + 2 × SD) of the values for HS.

$CD11c^{high}$ NK cells express HLA-DR more brightly than $CD11c^{low}$ NK cells

It was previously reported that infection with certain viruses would accompany up-regulation of CD11c on NK cells (16). This raises a possibility that the increased expression of CD11c in $CD11c^{high}$ MS may reflect an activation state of NK cells caused by some sort of stimuli. To verify this hypothesis, we examined surface expression of cell activation markers (CD69 and HLA-DR). Although CD69, an early activation marker, was not detectable on NK cells (Fig. 2*a*), NK cells from MS, particularly $CD11c^{high}$ MS, significantly overexpressed HLA-DR on surface (Fig. 2). Interestingly, HLA-DR expression was also up-regulated on $CD4^+$ T cells from $CD11c^{high}$ MS compared with those from HS (data not shown). These results indicate that NK cells and T cells are differentially activated in $CD11c^{high}$ MS, $CD11c^{low}$ MS, and HS.

Absence of NK2 bias in $CD11c^{high}$ MS

We have previously reported that a higher level of IL-5 expression (NK2 bias) is one of the characteristics of NK cells of MS in

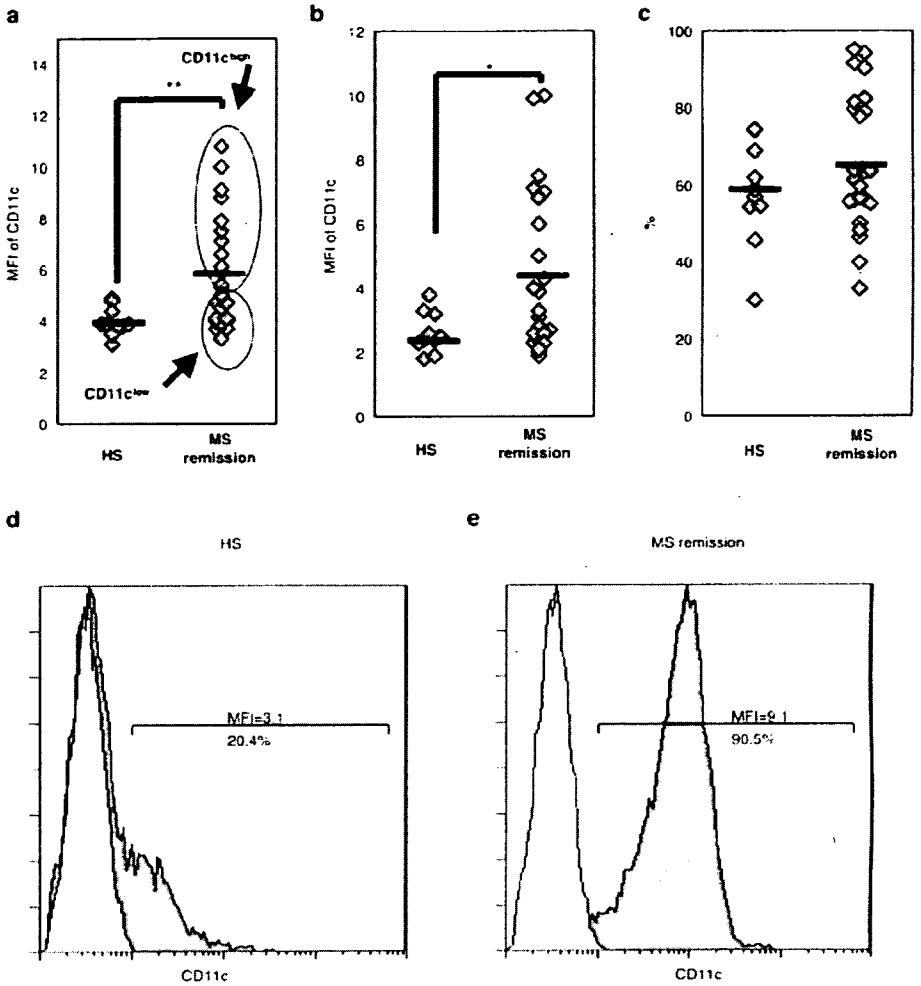

FIGURE 1. CD11c on NK cells is up-regulated in MS in remission. *a*, PBMC from HS ($n = 10$) and MS patients in remission ($n = 25$) were stained with anti-CD11c-PE, -CD3-ECD, and -CD56-PC5 mAb, and CD11c expression was measured on the $CD11c^+$ fraction gated within whole NK cells ($CD11c^+CD3^-CD56^+$ cells) as mean fluorescence intensity (MFI). Each dot represents the data from individual patients. $CD11c^{high}$ and $CD11c^{low}$ groups of patients are encircled as described in the text. *b*, In parallel, CD11c expression (MFI) was measured for the whole NK cells ($CD3^-CD56^+$ cells), which yielded a similar result. *c*, The proportions of $CD11c^+$ cells among whole NK cells are plotted. No significant difference was noted between HS and MS remission. *d* and *e*, Representative histogram patterns of CD11c on NK cells (closed histogram) from a single healthy subject (HS) (*d*) and a patient corresponding to $CD11c^{high}$ MS (*e*). Open histograms represent isotype control staining. Values represent proportions of $CD11c^+$ fraction (%) and MFI for $CD11c^+$ cells. Mann-Whitney *U* test was used for statistical analysis. Horizontal bars indicate the mean values. *, $p < 0.05$; **, $p < 0.01$.

remission (3). Although the mechanism for NK2 bias in MS remains to be further studied, up-regulation of GATA-3 has recently been reported in the induction of NK2 cells in mice (17). To explore the possible difference in the functions of $CD11c^{high}$ and $CD11c^{low}$ NK cells, we isolated NK cells from $CD11c^{high}$ or $CD11c^{low}$ group of patients and measured the mRNA levels of representative cytokines IFN-γ and IL-5 as well as corresponding transcription factors T-bet and GATA-3. As shown in Fig. 3, mRNA expression of both IL-5 and GATA-3 was significantly higher in $CD11c^{low}$ MS compared with HS or $CD11c^{high}$ MS, indicating that NK2 bias thought to be characteristic of MS remission is restricted to $CD11c^{low}$ MS. In contrast, there were no differences in mRNA expression of IFN-γ and T-bet among these three groups. Because NK cells from $CD11c^{high}$ patients expressed HLA-DR most brightly, we speculate that NK2 bias associated with $CD11c^{low}$ MS would attenuate when NK cells are further activated or differentiated.

NK cell stimulatory proinflammatory cytokines induce up-regulation of CD11c

We next attempted to explore the mechanism(s) for up-regulation of CD11c on NK cells in $CD11c^{high}$ MS. Because both NK cells and $CD4^+$ T cells overexpressed HLA-DR in $CD11c^{high}$, is it probable that immune signals influencing both innate and acquired immunity are operative. So we hypothesized that cytokine signals that have been implicated in the pathogenesis of MS may play a role. We cultured NK cells from HS in the presence or absence of cytokine(s) for 3 days, and evaluated the CD11c expression (MFI). We focused our attention to IL-12, IL-15, and IL-18, which are known to stimulate NK cells with or without help of other cytokines. Notably, they are reportedly elevated in the serum or blood lymphocytes of MS patients as compared with HS (11–14, 18, 19), and prior studies suggest that they may play an important role in autoimmune diseases (20–24). As shown in Fig. 4, although IL-12 and IL-18 showed only a marginal effect on purified NK cells, IL-15 consistently induced 2- to 3-fold up-regulation of CD11c compared with control culture without addition of cytokines. As IL-12 and IL-18 were reported to synergistically work in various settings (25, 26), we then examined whether combinations of these cytokines may induce CD11c. Combination of IL-15 and IL-12 or of IL-15 and IL-18 did not augment the CD11c expression to the level higher than that could be induced by IL-15 alone. However, the combination of IL-12 and IL-18 did up-regulate CD11c on NK cells, which was comparable to the effect of IL-15 alone (Table I). Additionally, we tested the effects of several cytokines involved in differentiation of DC (TNF-α, GM-CSF, IL-4) (27), or known to up-regulate CD11c in granulocytes (IL-8) as controls (28) in the same assay. These cytokines showed no significant effect (Table I).

$CD11c^{high}$ MS relapsed earlier

Given the significant difference in activation status and cytokine phenotype of NK cells as well as HLA-DR expression by $CD4^+$ T cells, it was particularly interesting to know whether $CD11c^{low}$ and $CD11c^{high}$ MS may follow a different clinical course. A new cohort of